

AD-A105 655

AIR FORCE WRIGHT AERONAUTICAL LABS WRIGHT-PATTERSON AFB OH F/G 13/8
SYNTHESIS, CHARACTERIZATION AND OPTICAL PROPERTIES OF BARIUM TI--ETC(U)
JUN 81 J C OLSON, D F STEVISON, I BRANSKY

UNCLASSIFIED

AFWAL-TR-81-4049

NL

1 x 1
AD-A
056411

END

GATE

FILED

11-81

DTIC

LEVEL

10

AFWAL-TR-81-4049



SYNTHESIS, CHARACTERIZATION AND OPTICAL PROPERTIES OF
BARIUM TITANATE FILMS SPUTTERED UNDER VARIOUS CONDITIONS

Laser Hardened Materials Branch
Electromagnetic Materials Division

June 1981

DTIC

OCT 14 1981

H

Final Report for Period 1 April 1980 - 5 December 1980

Approved for public release; distribution unlimited.

DTIC FILE COPY

MATERIALS LABORATORY
AIR FORCE WRIGHT AERONAUTICAL LABORATORIES
AIR FORCE SYSTEMS COMMAND
WRIGHT-PATTERSON AIR FORCE BASE, OHIO 45433

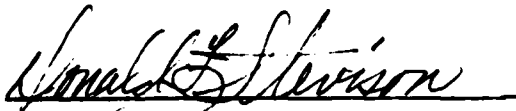
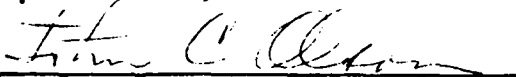
AD A105655

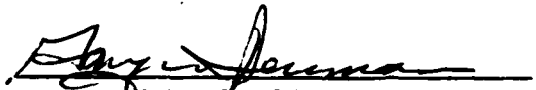
NOTICE

When Government drawings, specifications, or other data are used for any purpose other than in connection with a definitely related Government procurement operation, the United States Government thereby incurs no responsibility nor any obligation whatsoever; and the fact that the government may have formulated, furnished, or in any way supplied the said drawings, specifications, or other data, is not to be regarded by implication or otherwise as in any manner licensing the holder or any other person or corporation, or conveying any rights or permission to manufacture, use, or sell any patented invention that may in any way be related thereto.


This report has been reviewed by the Information Office (OI) and is releasable to the National Technical Information Service (NTIS). At NTIS, it will be available to the general public, including foreign nations.

This technical report has been reviewed and is approved for publication.


GARY L. DENMAN, Chief
Laser Hardened Materials Branch
Electromagnetic Materials Division

FOR THE COMMANDER


MERRILL L. MINGES, Chief
Electromagnetic Materials Division
Materials Laboratory

"If your address has changed, if you wish to be removed from our mailing list, or if the addressee is no longer employed by your organization please notify AFWAL/MLPJ, W-PAF8, OH 45433 to help us maintain a current mailing list".

Copies of this report should not be returned unless return is required by security considerations, contractual obligations, or notice on a specific document.

REPORT DOCUMENTATION PAGE		READ INSTRUCTIONS BEFORE COMPLETING FORM
1. REPORT NUMBER AFWAL-TR-81-4049	2. GOVT ACCESSION NO.	3. RECIPIENT'S CATALOG NUMBER
4. TITLE (and Subtitle) SYNTHESIS, CHARACTERIZATION AND OPTICAL PROPERTIES OF BARIUM TITANATE FILMS SPUTTERED UNDER VARIOUS CONDITIONS.	5. TYPE OF REPORT & PERIOD COVERED Final Report, for Period 1 Apr 81 - 5 Dec 80	6. PERFORMING ORG. REPORT NUMBER
7. AUTHOR(s) John C. Olson Donald F. Stevison Izhar Bransky	8. CONTRACT OR GRANT NUMBER(s)	
9. PERFORMING ORGANIZATION NAME AND ADDRESS Materials Laboratory (AFWAL/MLPJ) Air Force Wright Aeronautical Laboratories Wright-Patterson Air Force Base, Ohio 45433	10. PROGRAM ELEMENT, PROJECT, TASK AREA & WORK UNIT NUMBERS 2422 242204 01 62102F	
11. CONTROLLING OFFICE NAME AND ADDRESS Materials Laboratory (AFWAL/ML) Air Force Wright Aeronautical Laboratories Wright-Patterson Air Force Base, Ohio 45433	12. REPORT DATE Jun 1981	13. NUMBER OF PAGES 73
14. MONITORING AGENCY NAME & ADDRESS (if different from Controlling Office)	15. SECURITY CLASS. (of this report) Unclassified	15a. DECLASSIFICATION DOWNGRADING SCHEDULE
16. DISTRIBUTION STATEMENT (of this Report) Approved for public release; distribution unlimited.		
17. DISTRIBUTION STATEMENT (of the abstract entered in Block 20, if different from Report)		
18. SUPPLEMENTARY NOTES		
19. KEY WORDS (Continue on reverse side if necessary and identify by block number)		
BaTiO ₃ (Barium Titanate)	Density	Phase transition
Sputter film growth rate	X-ray diffraction	Surface temperature
Transmission spectrophotometry	Dielectric constant	Electrical Conductivity
Ferroelectric material	Index of refraction	Band gap energy
20. ABSTRACT (Continue on reverse side if necessary and identify by block number)		
<p>Data is presented on BaTiO₃ films which were rf sputtered on Pt, quartz and sapphire substrates at various temperatures and gas mixtures. Measurements of density, dielectric constant, electrical conductivity, X-ray diffraction, energy band gap from optical absorption and wavelength, and temperature dependence of refractive index are presented. Measurements were also made on a BaTiO₃ single crystal and a hot-pressed ceramic pellet for direct comparison of bulk properties to those of the films.</p> <p>(Continued on back)</p>		

Block 20. ABSTRACT

The results of this work demonstrate that a transition of the properties occurs between the amorphous and crystalline states depending on the surface temperature during sputtering. The transition is sluggish up to 700°C above which crystalline properties of the films appear rapidly.

↑

FOREWORD

This report was prepared by the Laser Hardened Materials Branch of the Materials Laboratory, Air Force Wright Aeronautical Laboratories. Part of the described work was performed under Project 2422, Task 242204, with Mr. Donald F. Stevison and Mr. John C. Olson as the AFWAL/MLPJ Project Engineers. Dr. I. Bransky was a visiting scientist at AFWAL/MLPJ, under Contract F33615-79-C-5129, Universal Energy Systems, Dayton, Ohio, during the period April-December 1980.

We, the authors, are most grateful to our colleagues in the Materials Laboratory who helped us to carry out various physical measurements. In particular, Ms. Debra Edwards for running many experimental determinations on the index of refraction, Captain James Mosora, who ran idealized curves on a computer for comparisons to the experimental data, Charles Strecker who ran the early ellipsometric measurements and parabolic curve fits of the experimental data, Dr. Moshe Ish-Shalom who provided the X-ray analysis, and Everett Rea of the Illinois Institute of Technology Research Institute (IITRI) who provided the absorption edge data. Also, Kent Kogler of IITRI was very helpful in many technical discussions. A special acknowledgement goes to Dr. C. H. Perry of the Physics Department of Northeastern University who supplied us with the large single crystal of BaTiO_3 .

Accession For	
NTIS GRA&I	<input checked="checked" type="checkbox"/>
DTIC TAB	<input type="checkbox"/>
Unannounced	<input type="checkbox"/>
Justification	
By _____	
Distribution/	
Availability Codes	
Dist	Avail and/or Special
A	

TABLE OF CONTENTS

SECTION	PAGE
I INTRODUCTION	1
II EXPERIMENTAL	4
1. Sputtering System	4
2. Substrates	4
3. Optimizing Sputtering Conditions	6
4. Measurements of Film Growth Rate	8
5. Measurements of Substrate Surface Temperatures During Sputtering	8
6. Film Density Measurements	16
7. SEM and EDAX Examinations	16
8. X-ray Diffraction Analysis	16
9. Dielectric Constant and Electrical Conductivity Measurements	16
10. Transmission Spectrophotometry of BaTiO ₃ Films	17
III RESULTS	20
1. Rate of BaTiO ₃ Growth as a Function of the Sputtering Power	20
2. Dielectric Constants and Electrical Conductivity	20
3. Transmission Spectra and Absorption Edge	24
4. Density Measurements	30
5. X-ray Diffraction	32
6. Index of Refraction Measurements	35
a. Method of Index Measurements	35
b. Optical System for Index Measurements	38
c. Results of Refractive Index Measurements	41

TABLE OF CONTENTS (Concluded)

SECTION	PAGE
IV SUMMARY AND CONCLUSION	56
V SUGGESTIONS FOR FURTHER WORK	61
REFERENCES	63

LIST OF ILLUSTRATIONS

FIGURE		PAGE
1	Sputtering System	5
2	Thickness Profiles of BaTiO ₃ Films Sputtered Under Various Conditions	7
3	Platinum Resistance Thermometer for Measuring Substrate Surface Temperature During Sputtering	9
4	Platinum Resistance Thermometer Calibration	11
5	Rate of Increase of Substrate Surface Temperature at Various Sputtering Power Levels for Unpreheated Substrates	12
6	Rate of Increase of Substrate Surface Temperature at Various Sputtering Power Levels for Preheated Substrates	13
7	Equilibrium Surface Temperature as a Function of Sputtering Power for Unpreheated and Preheated Substrates	14
8	Determination of the Dielectric Constant from Capacitance vs. Contact Area	15
9	Dielectric Constant of a Ceramic BaTiO ₃ Pellet as a Function of Temperature	18
10	IR Transmission Spectra of a Sapphire Substrate, BaTiO ₃ Film and a Single Crystal of BaTiO ₃	19
11	Rate of BaTiO ₃ Film Growth as a Function of the Sputtering Power	21
12	Typical Transmittance in the Vicinity of the Absorption Edge for BaTiO ₃ Films and a Single Crystal	26
13	Determination of Band Gap Energy, E_g , from α^2 vs. $h\nu$	27
14	Determination of Band Gap Energy, E_g , from $\sqrt{\alpha h\nu}$ vs. $h\nu$	28
15	X-ray Diffraction Intensity vs. Diffraction Angle for Films and the Ceramic BaTiO ₃ Pellet	33
16	Variation of Reflectivity with Angle of Incidence for Substrates and for Films of Various Thicknesses	34
17	Computed Relative Reflectivity vs. Incidence Angle for a Film on a Substrate with Index of 1.7	39

LIST OF ILLUSTRATIONS (Concluded)

FIGURE		PAGE
18	Computed Relative Reflectivity vs. Incidence Angle for a Film on a Substrate with Index of 1.5	40
19	Refractive Index of BaTiO ₃ Films, Ceramic Pellet, and Single Crystal vs. Wavelength at Room Temperature	48
20	Relative Reflectivity vs. Incidence Angle of BaTiO ₃ Ceramic Pellet at 404 nm and 632.8 nm	49
21	Relative Reflectivity vs. Incidence Angle of an Amorphous BaTiO ₃ Film on Sapphire at 404 nm	50
22	Relative Reflectivity vs. Incidence Angle of an Amorphous BaTiO ₃ Film on Sapphire at 632.8 nm	51
23	Relative Reflectivity vs. Incidence Angle of an Amorphous BaTiO ₃ Film on Sapphire at 436 nm	52
24	Relative Reflectivity vs. Incidence Angle of BaTiO ₃ Film on Sapphire Sputtered at ~800°C Surface Temperature at Two Wavelengths	53
25	Temperature Dependence of Average Refractive Index of a BaTiO ₃ Ceramic Pellet (Xenon Light Source, No Filter)	54
26	Relative Reflectivity vs. Incidence Angle of a BaTiO ₃ Film on Sapphire Sputtered at ~1000°C Surface Temperature	55

LIST OF TABLES

TABLE		PAGE
1	Deposition Rates of Sputtered BaTiO ₃ Films as a Function of the Sputtering Power for Various Gas Mixtures and Substrate Temperatures	22
2	Electrical Properties of Sputtered BaTiO ₃ Films	23
3	Absorption Edge Energy Gap for BaTiO ₃ Films Sputtered Under Various Conditions and a BaTiO ₃ Single Crystal	29
4	Apparent Density of BaTiO ₃ Films Sputtered Under Various Conditions on Quartz and Sapphire Substrates in 15 mTorr Total Pressure	31
5	Refractive Index of BaTiO ₃ Single Crystal in the Spectral Range 400-590 nm	42
6	Refractive Index of BaTiO ₃ Hot Pressed Ceramic Pellet in the Spectral Range 404-632.8 nm	43
7	Refractive Index of BaTiO ₃ Film, 5320 Å Thick, Sputtered at 300 Watts on Sapphire Preheated to 620°C in 5% O ₂ /95% Ar (15 mTorr)	44
8	Refractive Index of BaTiO ₃ Film, 4800 Å Thick, Sputtered at 100 Watts on Sapphire Preheated to 580°C in 5% O ₂ /95% Ar (15 mTorr)	45
9	Refractive Index of Amorphous BaTiO ₃ Film, 4550 Å Thick, Sputtered at 300 Watts on Sapphire Not Preheated in Pure Argon (15 mTorr)	46
10	Temperature Dependence of the Refractive Index of a BaTiO ₃ Ceramic Pellet Using a Xenon Light Source	47
11	Summary of the Physical Constants of Various Forms of BaTiO ₃	58

SECTION I

INTRODUCTION

Crystalline barium titanite (BaTiO_3) is known to undergo a series of phase transformations. On cooling, its crystal structure goes from cubic to tetragonal at 120°C , tetragonal to orthorhombic at 0°C and orthorhombic to rhombohedral at -90°C . In the tetragonal phase, there is an opposite shift of the titanium and oxygen sublattices so that for this phase, at approximately 0°C , the lattice parameters are $a = 3.990 \text{ \AA}$ and $c = 4.035 \text{ \AA}$ ($\frac{c}{a} - 1 = 0.0113$). In the cubic phase, crystalline as well as polycrystalline BaTiO_3 is paraelectric, while it is ferroelectric in the tetragonal phase. At the Curie temperature, 120°C , the dielectric constants vs. temperature curve shows a sharp peak. For polycrystalline specimens, the magnitude of the relative dielectric constant at the peak is 12,000-4000 and 2500-200 at room temperature (Reference 1). Crystalline tetragonal BaTiO_3 has a dielectric constant of 200 in the c direction and 4000 in the a direction at room temperature.

BaTiO_3 crystals are birefringent. The refractive index of BaTiO_3 had been studied on single crystals only. The average value of the two principle indices for single ferroelectric domain crystals is reported to be 2.40 at room temperature in the visible [$n_o = 2.428$, $n_e = 2.371$ (λ_{Na}) (Reference 2)]. A jump of 1.3% is found for the ordinary n at the Curie temperature, $n_o = 2.368$ to 2.398 for $\lambda = 589.3 \text{ nm}$ (Reference 3).

This behavior of the index is in accordance with Mott's relation

$$n^2 < \epsilon < DK_\infty \quad (1)$$

where n is the refractive index, ϵ is the dielectric constant and DK_∞ is the static dielectric constant (Reference 4). Optical changes of the refractive index by intense laser flux were reported in BaTiO_3 single crystals (Reference 5).

The production and dielectric properties of BaTiO_3 thin films were studied by many investigators because of their potential application as a high dielectric constant material in microelectronic elements of high capacitance per unit area. Films of BaTiO_3 were produced with various vacuum techniques of which rf sputtering appears to be the most reproducible method.

It has been reported that both amorphous and tetragonal BaTiO_3 films can be produced by rf sputtering depending on the substrate temperature and ratio of oxygen to argon. The latter controls the stoichiometry of the film. Rf sputtering in pure argon on substrates held at room temperature resulted in BaTiO_3 films which showed no crystalline patterns in the X-ray diffraction, i.e., amorphous films (Reference 5). The relative dielectric constant of such films was low, in the range of 10-20 (Reference 6).

When BaTiO_3 is sputtered in an oxygen/argon mixture (about 5% oxygen/95% argon) on substrates held at temperatures above $\sim 600^\circ \text{C}$, X-ray diffraction patterns of the films show an amount of tetragonal crystalline structure (Reference 7 and 8). The dielectric constant increases by an order of magnitude. The higher the substrate temperature, the larger the amount of tetragonal phase observed. Sputtering on substrates at temperatures up to 1000°C were reported (Reference 7).

In the framework of studying the behavior of optical parameters of materials undergoing phase transformations, the present work was aimed at studying the optical parameters of ferroelectric films, specifically of sputtered BaTiO_3 in the region of the tetragonal to cubic transformation. The main objective was to investigate the dependence of the refractive index of sputtered BaTiO_3 films on various sputtering conditions. Various material characterizations were undertaken to establish correlations of optical properties to other physical parameters. The dielectric constant and electrical conductivity were measured because their magnitude is a very sensitive property of the state of BaTiO_3 films or bulk material. In addition, apparent densities were measured for various sputtering conditions to determine film compactness.

Other measurements included spectrophotometric measurements of film absorption and reflection, refractive index, scanning electron microscopy and X-ray diffraction. All of the above measurements in thin BaTiO_3 films were also conducted for comparison on hot pressed ceramic* and single crystal** samples. This provides information for comparison of thin films to the bulk and sets an upper limit for values expected from the thin films.

* Provided by K. S. Mazdiasni, AFWAL/MLLM.

** Provided by Dr. Perry of Northeastern University.

SECTION II

EXPERIMENTAL

In the present study, BaTiO_3 films were produced under several conditions: amorphous films--sputtered in argon on substrates not preheated (later referred to as room temperature); and tetragonal films--sputtered in a mixture of 5% oxygen/95% argon on substrates preheated to 600° C or to 800° C.

1. THE SPUTTERING SYSTEM

The sputtering system used in these studies was an R. F. Sputter-Etch Module, model SEM-8620 manufactured by Material Research Corporation in Orangeburg, New York. The unit was operated in the diode rf sputtering mode for all film dispositions, as opposed to the rf bias sputtering mode. A fully rotatable triple shutter design provides full protection of substrates and unused targets during sputtering operations and contamination protection of targets during etch operations.

A "J"-shaped rotatable, water-cooled assembly, as shown in Figure 1, acts as either an anode or cathode and does double duty as an etch platform and substrate holder.

The target used for these experiments was "MARZ" grade (99.99%) sintered ceramic disc of BaTiO_3 150 mm diameter and 4 mm thick. Substrates could be heated during deposition by an electric plate heater up to 800° C.

2. SUBSTRATES

Three types of substrates were used in the present study:

- a. Optically polished sapphire discs, 25 mm in diameter, 1.5 mm thick.
- b. Optically polished quartz plates 3 mm thick and about 20 x 20 mm. Quartz and sapphire substrates for refractive index measurements were abraded on one side.

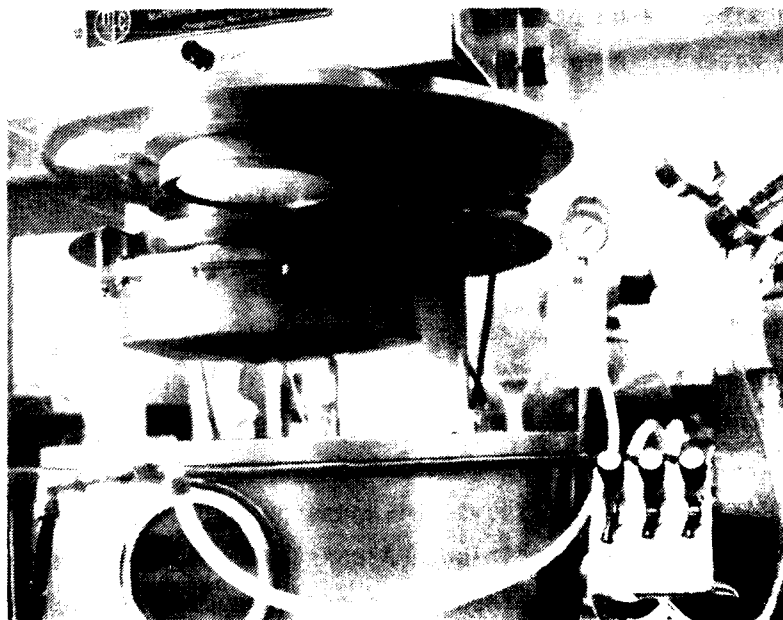
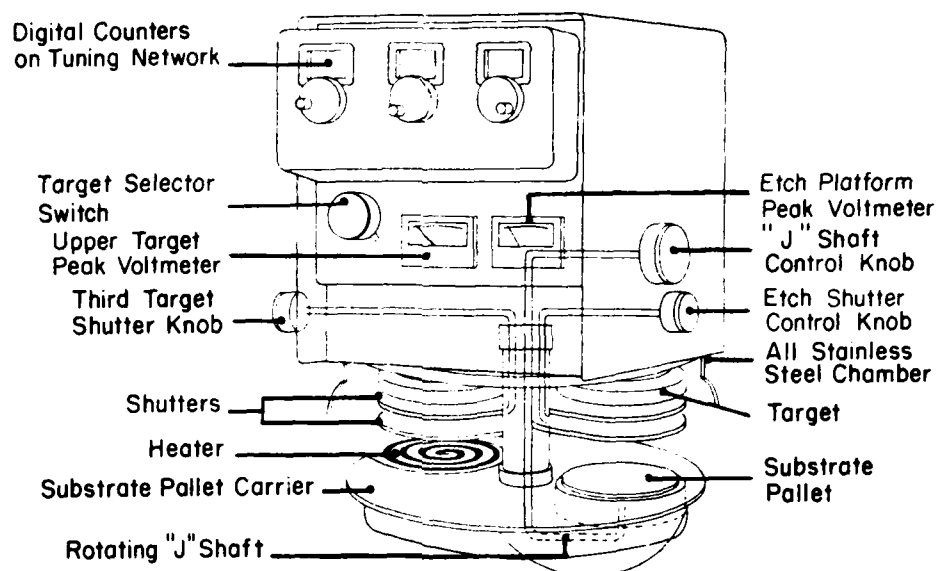


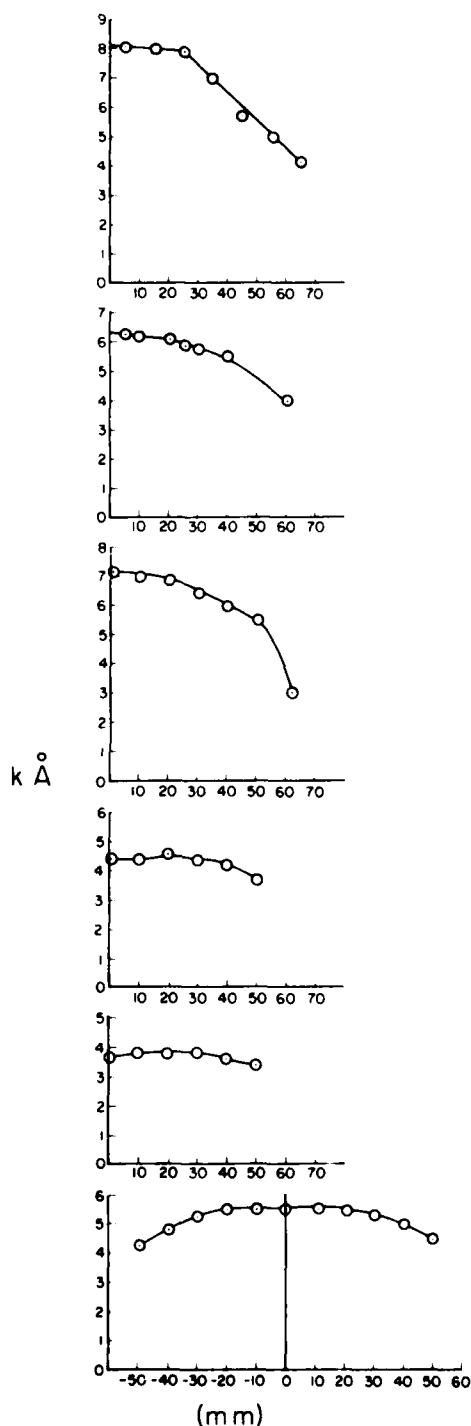
Figure 1. Sputtering System

- c. 0.25 mm thick platinum foils about 12 x 25 mm. The platinum foils were polished with Buehler's 6, 3 and 1 micron diamond polish paste and 0.3 to 0.05 micron alumina powder micropolish.

Substrates went through three stages of ultrasonic cleaning: Alcanox, distilled water and ethyl alcohol.

3. OPTIMIZING SPUTTERING CONDITIONS

In order to establish sputtering conditions for films of uniform thickness distribution, the thickness of amorphous films sputtered on quartz and sapphire substrates was measured as a function of anode to cathode distance and of argon total pressure at various sputtering power levels. The anode plane was a copper pallet on a water cooled platform. The sputtered film thickness was determined by measuring the height of a step etched in the film using stylus instruments. A "Dektak" and a "Tallysurf" surface profile measuring system were used to measure step heights. Well-defined steps were obtained on both quartz and sapphire by etching the BaTiO_3 with Kroll's solution (5% HF, 10% HNO_3 + water). Prior to etching, a strip of the film was masked with mylar tape and then the entire film was coated with Apiezon wax. Removing the tape exposed the film to etching. The wax was removed later with trichloroethylene and the film was cleaned with ethanol. Since ultrasonic cleaning removes pieces of the film, it was not used. Thickness measurements were reproducible to within 2% on both instruments. Interference thickness measurements with a M-10 Angstrometer confirmed the stylus instruments measurements. The best results for Angstrometer measurements were obtained for films with steps coated (by sputtering) with a platinum film. This produced high contrast interference fringes across the step. Figure 2 shows thickness profiles of BaTiO_3 films sputtered under various condition. A constant thickness region of about 60 mm diameter is obtained at an anode to cathode distance of 30 mm (substrates were 3 mm thick) and for an argon pressure of 15 mTorr independent of sputtering power in the range from 50 to 300 watts (rf voltage 460-1100 volts). Film thickness within the 60 mm diameter



Run 0137; P: 100W, t: 240min,
Ar p: 7.5mTorr,
Target-sub. d: 43mm.

Run 0141; P: 50W, t: 340min,
Ar p: 7.5mTorr,
Target-sub. d: 36mm.

Run 0142; P: 200W, t: 120min,
Ar p: 7.5mTorr,
Target-sub. d: 36mm.

Run 0143a; P: 200W, t: 100min,
Ar p: 7.5mTorr,
Target-sub. d: 30mm.

Run 0143b; P: 200W, t: 70min,
Ar p: 15.0mTorr,
Target-sub. d: 30mm.

Run 0144; P: 100W, t: 183min,
Ar p: 15.0mTorr,
Target-sub. d: 30mm.

Figure 2. Thickness Profiles of BaTiO_3 Films Sputtered Under Various Conditions

were constant within the experimental error of thickness determination (i.e. within ~2 %). During all further sputtering of BaTiO_3 films, substrates were placed within the 60 mm region of constant thickness. All sputtered films looked transparent, homogeneous and flawless.

To clean its surface, the BaTiO_3 target was always presputtered at 250 watts for about 10 minutes prior to the sputtering run. After sputtering at high temperature, the substrates were cooled at a rate of 7-8 °C/min to room temperature. This was done to prevent cracking of the film due to the different thermal expansion of film and substrate.

4. MEASUREMENTS OF FILM GROWTH RATE

In the fixed 30 mm anode to cathode spacing, the rate of film growth was measured as a function of sputtering power in pure argon and in a mixture of 5% oxygen/95% argon, both at a total pressure of 15 mTorr. Identical results were found for quartz and sapphire substrates as is discussed in Section III "Results": However, the rate of growth on platinum foils was found to be considerably lower. Unlike the quartz and sapphire, the platinum foils were maintained at ground potential and at room temperature due to superior electrical and thermal conduction.

5. MEASUREMENTS OF SUBSTRATE SURFACE TEMPERATURE DURING SPUTTERING

Since film properties are strongly dependent on substrate surface temperature during deposition, it was desired to determine the temperature of the substrate surface during sputtering. Quartz and sapphire are poor heat conductors and their surface temperature during sputtering was expected to be higher than the cooled copper pallet. The resistance change of a platinum film deposited on a 3 mm thick quartz plate was used to monitor the surface temperature while BaTiO_3 was sputtered on it at various power levels*. The platinum thermometer is shown in Figure 3. Four holes were drilled in the quartz plate and were painted with platinum paint (Hanovia liquid bright platinum).

*The RF power was momentarily switched off during measurement.

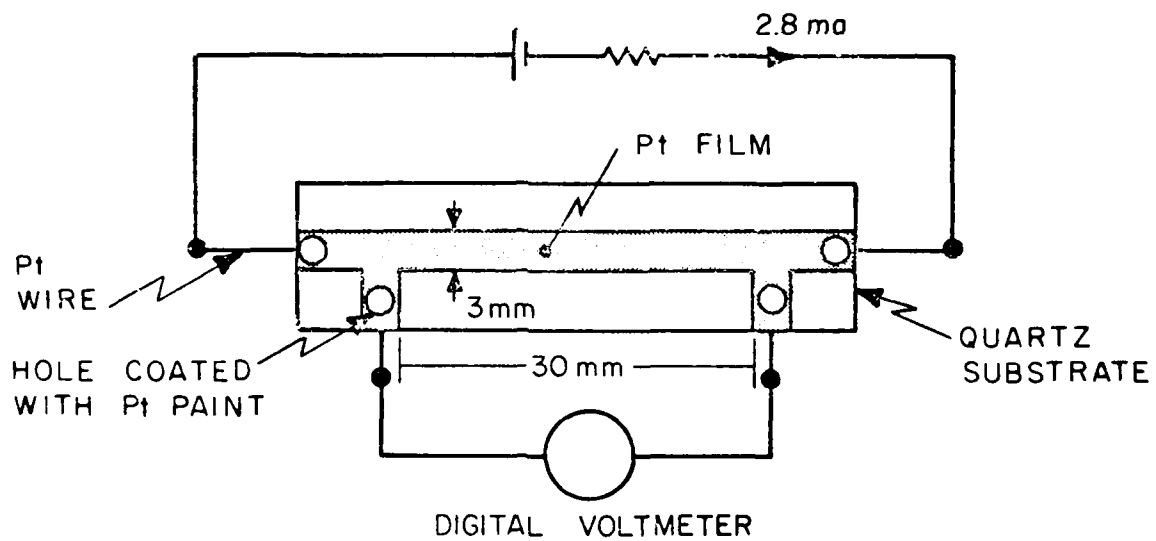


Figure 3. Platinum Resistance Thermometer for Measuring Substrate Surface Temperature During Sputtering

Thin platinum wires (0.1 mm) were then wrapped through the holes. A platinum film of $\sim 2000 \text{ \AA}$ was then sputtered on the quartz substrate using a mask. Calibration of the platinum film thermometer was made at 0° C (ice + water mix), 100° C (boiling water) and up to 300° C against an accurate thermocouple. The calibration graph is given in Figure 4. The thermometer equation for constant current of 2.8 ma is given in Equation 2.

$$T(^{\circ}\text{C}) = 43.5 \times V(\text{mv}) - 548 \quad (2)$$

This gives a temperature sensitivity of $0.023 \text{ mv}/^{\circ}\text{C}$.

Measurements of substrate temperature during sputtering in 15 mTorr argon pressure were made at various power levels in the range of 50 to 300 watts sputtering power. After approximately 10 minutes the quartz substrate surface reached equilibrium (see Figure 5). The substrate upper surface temperature differs appreciably from the water cooled base temperature (15° C) and it increases rapidly with the power (see Figure 7). Investigators using sputtering techniques are usually referring to the base temperature as substrate temperature not realizing the large discrepancy for substrates of low heat conduction.

The surface temperature during sputtering on a preheated quartz substrate was also measured by the same method. A 5% O_2 /95% Ar mixture at 15 mTorr was used and the sputtering power level was varied from 50 to 300 watts. The substrate (platinum resistance thermometer) was preheated to 615° C . Temperature vs. sputtering time plots are presented in Figure 6. Equilibrium is still reached after about 10 minutes. Note that the upper surface substrate temperature at 300 watts is considerably higher than the pallet temperature.* This "true" temperature (see Figure 7) has a marked effect on the resulting film properties. Figure 7 gives the surface equilibrium temperature for both unpreheated and preheated (615° C) quartz substrates.

* One surface temperature determination was made for preheating to 800° C at 300 watts sputtering power. In this case the surface temperature reached close to 1000° C .

$$T (^{\circ}\text{C}) = 43.5 \times V(\text{mV}) - 548$$

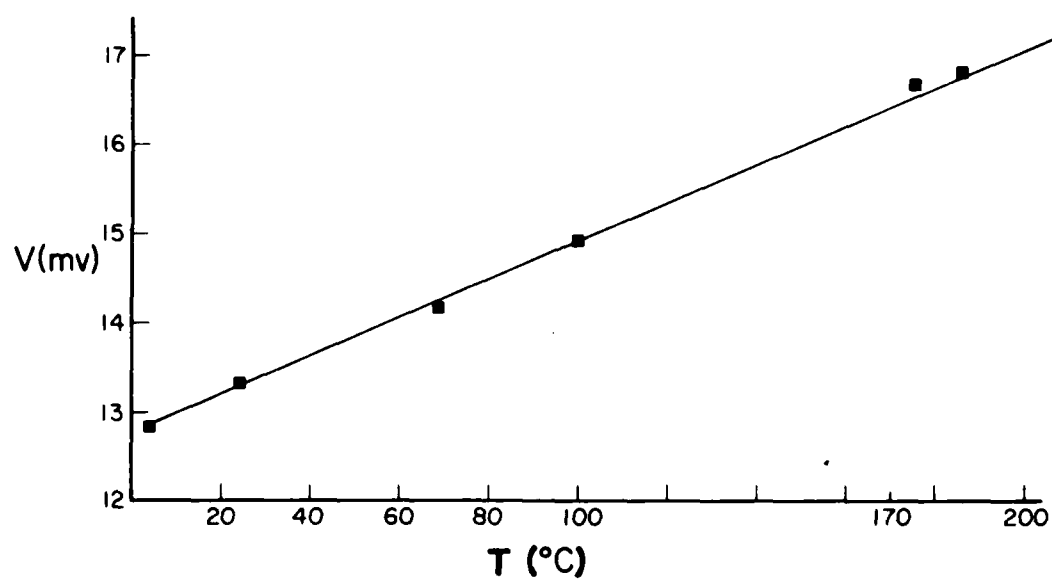


Figure 4. Platinum Resistance Thermometer Calibration

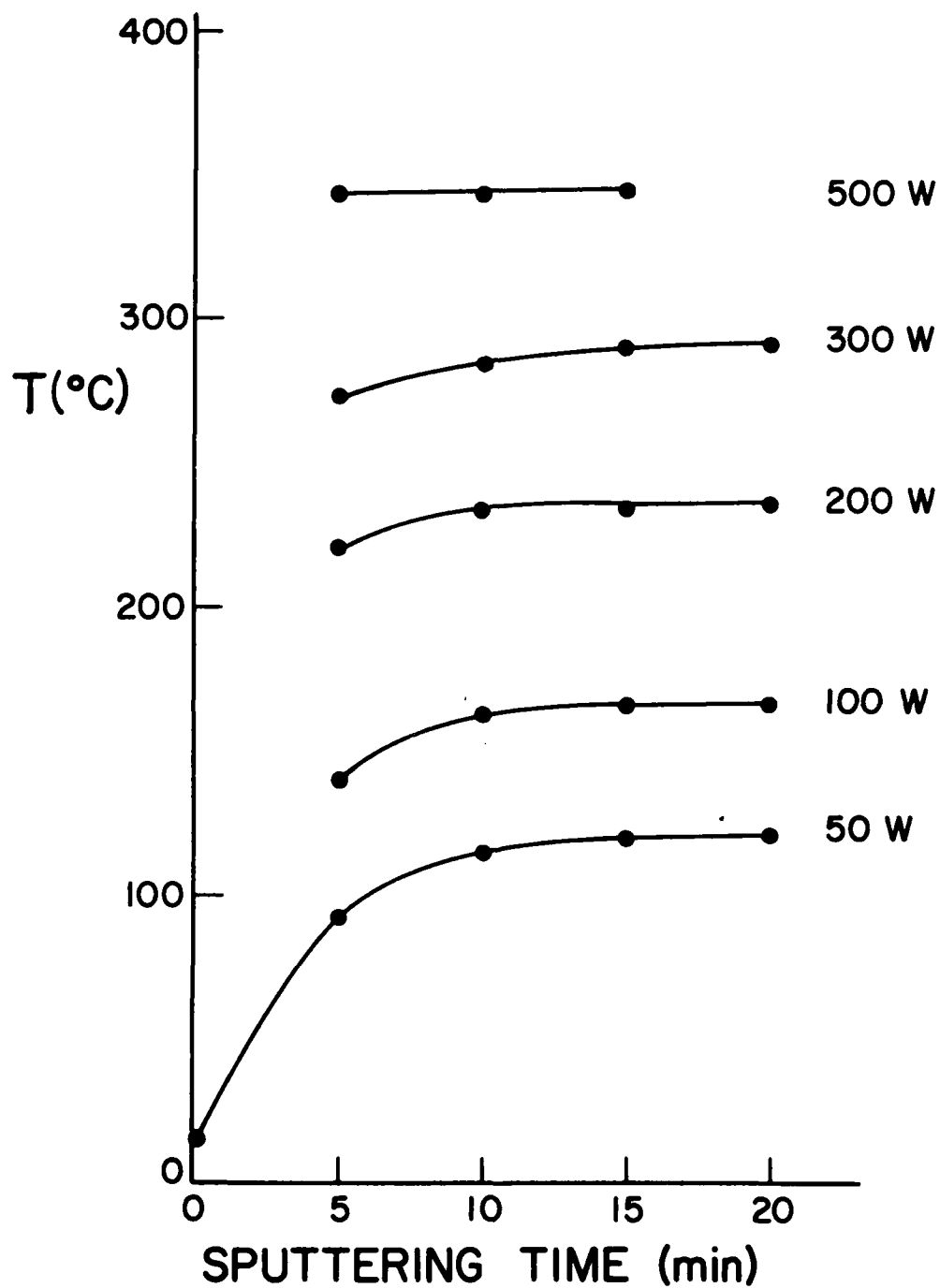


Figure 5. Rate of Increase of Substrate Surface Temperature at Various Sputtering Power Levels for Unpreheated Substrates

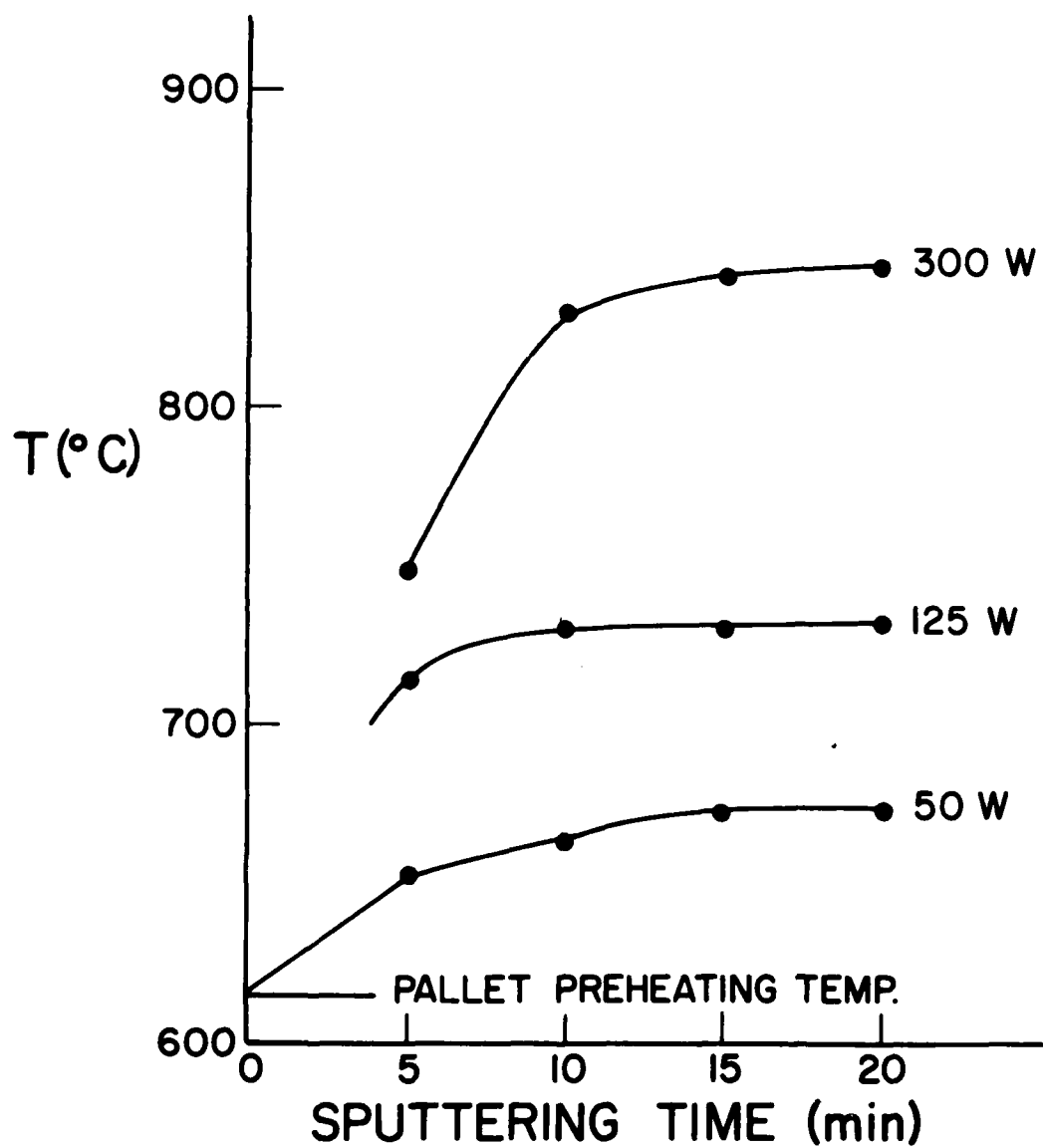


Figure 6. Rate of Increase of Substrate Surface Temperature at Various Sputtering Power Levels for Preheated Substrates

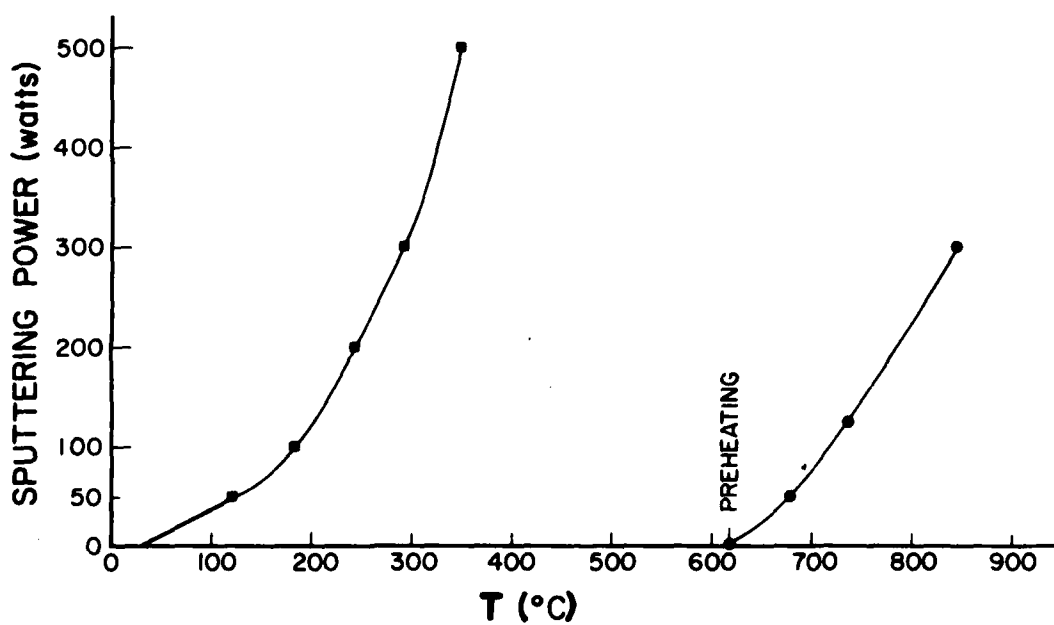


Figure 7. Equilibrium Surface Temperature as a Function of Sputtering Power for Unpreheated and Preheated Substrates

6. FILM DENSITY MEASUREMENTS

The apparent density of sputtered BaTiO_3 films on quartz and sapphire was calculated from the added weight and the thickness after deposition and the substrate area. A concentric alumina ring was placed around the sapphire disc and four quartz bars were placed along the sides of the quartz plate to prevent deposition on the substrate sides.

The added weight was determined by a Mettler microbalance. The overall error in the density measurement is estimated to be within 5% ($\pm 2.5\%$). In each run, the apparent film density was determined both on quartz and on sapphire. The agreement was within 2%.

7. SEM AND EDAX EXAMINATIONS

Films of various thicknesses deposited at various rates on platinum foils were examined with Scanning Electron Microscopy (SEM). SEM at 5K and 10K magnifications showed the films on platinum to be homogeneous, smooth and flawless. No pores were revealed at that magnification. EDAX showed only Ba and Ti characteristic lines with no other contribution.

8. X-RAY DIFFRACTION ANALYSIS

X-ray diffraction intensity ($\text{Cu}_{K\alpha}$) vs. diffraction angle were measured for amorphous, partially crystalline films and the ceramic hot pressed reference. Lattice parameters were calculated using a least squares fit to the characteristic diffraction lines.

9. DIELECTRIC CONSTANT AND ELECTRICAL CONDUCTIVITY MEASUREMENTS

The dielectric constants of the BaTiO_3 films and a ceramic hot pressed pellet were measured with a Hewlett Packard automatic capacitance bridge, model 4270 A, which operates at 1.0 KHz and 1.0 V test voltage. The platinum foil served as one plate of the capacitor. The other plate was a conductive contact applied on the film.

Platinum contacts applied by sputtering were usually shorted probably due to film porosity, which was less than a 1000 Å in accordance with the SEM results. Even unshorted contacts could not be considered reliable because possible metal penetration might alter film electrical properties. The best way to apply unshorted contacts independent of their size (contacts up to 8 mm² were tested) was to apply a viscous conductive paste. A silver conductive epoxy was used. A series of four contacts of known area, A, from 1 to 7.5 mm² were applied through a mask. The dielectric constant, ϵ , was determined from the slope ϵ/d of the capacitance, C, vs. A, ($C = \epsilon \frac{A}{d}$), where d is the film thickness. The temperature dependence of ϵ was determined at room temperature using a sample holder with spring loaded contacts against a teflon base. The electrical conductivity, σ , was determined in a similar way from the slope of R^{-1} (as measured by the bridge) vs. A, since $R^{-1} = (\sigma/d)A$. Here R is the electrical resistance.

A typical C vs. A plot is shown in Figure 8. The results of the dielectric constant measurements on the ceramic pellet are presented in Figure 9. Pellet thickness was 2.67 mm and diameter 13.46 mm. Contacts were made with Hanovia liquid bright gold.

10. TRANSMISSION SPECTROPHOTOMETRY OF BaTiO₃ FILMS

BaTiO₃ films on optically polished transparent quartz and sapphire and a 1 mm thick single crystal were examined with a Perkin-Elmer model 621 spectrophotometer in the range of 2.5 to ~50 μm and with a Varian Cary 14 spectrometer in the range 200 nm - 2.5 μm. Figure 10 shows a typical transmission spectra. The energy gap, E_g , was calculated from the sharp absorption edge found in the range 250 - 400 nm.

$$\frac{\epsilon}{d} = \frac{215}{4} = 53.75 \frac{\text{PF}}{\text{mm}^2}$$

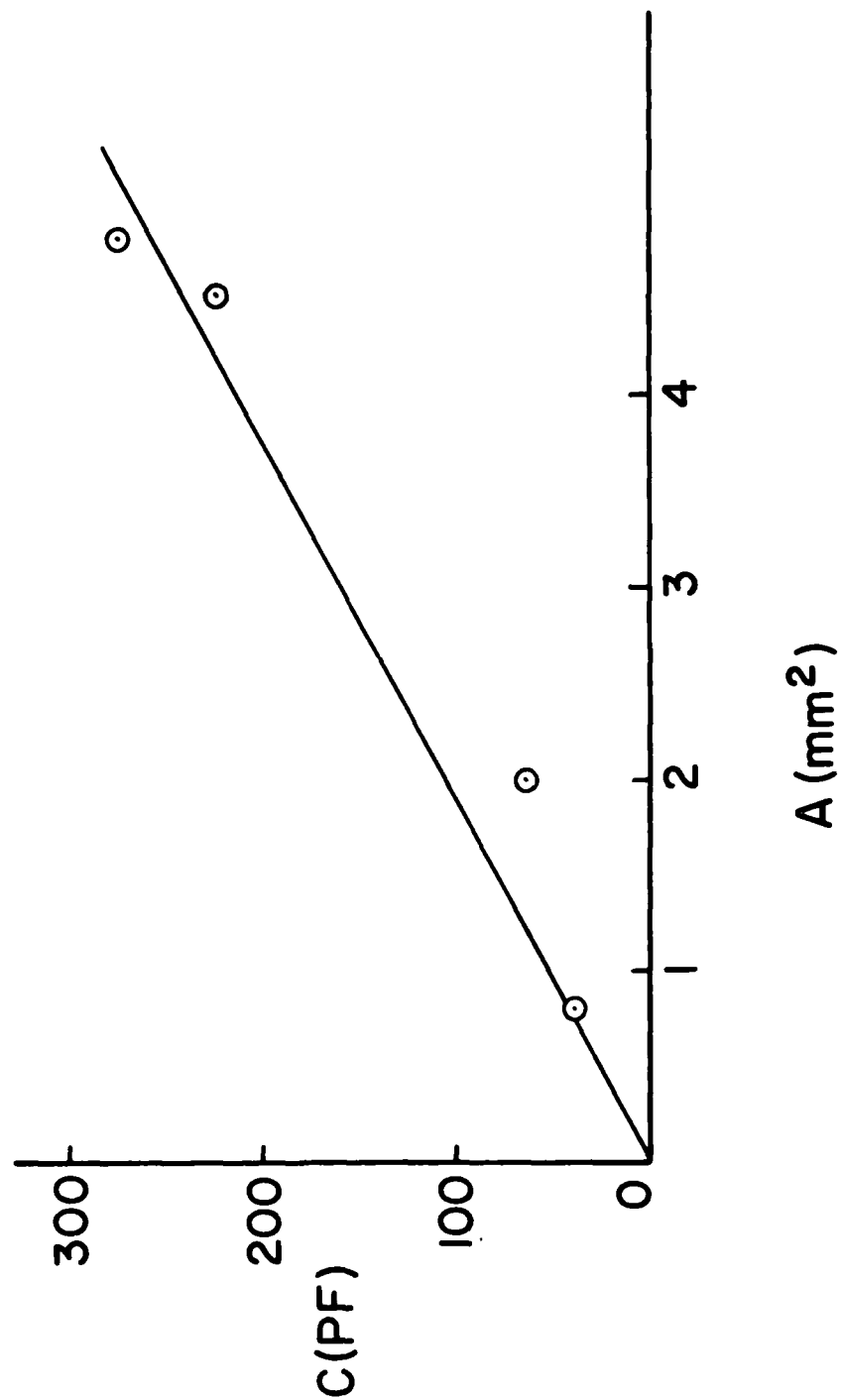


Figure 8. Determination of the Dielectric Constant from Capacitance vs. Contact Area

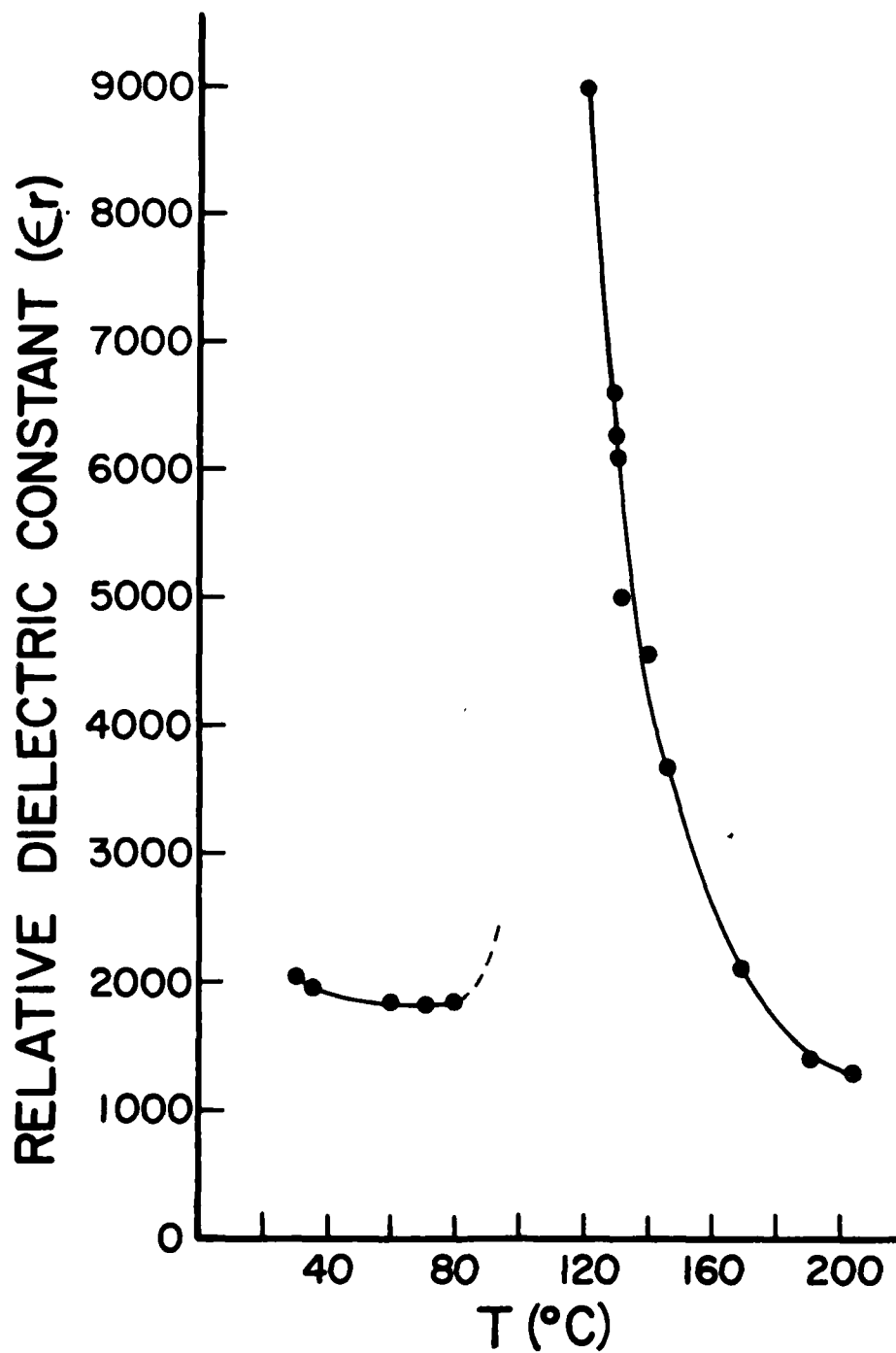


Figure 9. Dielectric Constant of a Ceramic BaTiO_3 Pellet as a Function of Temperature

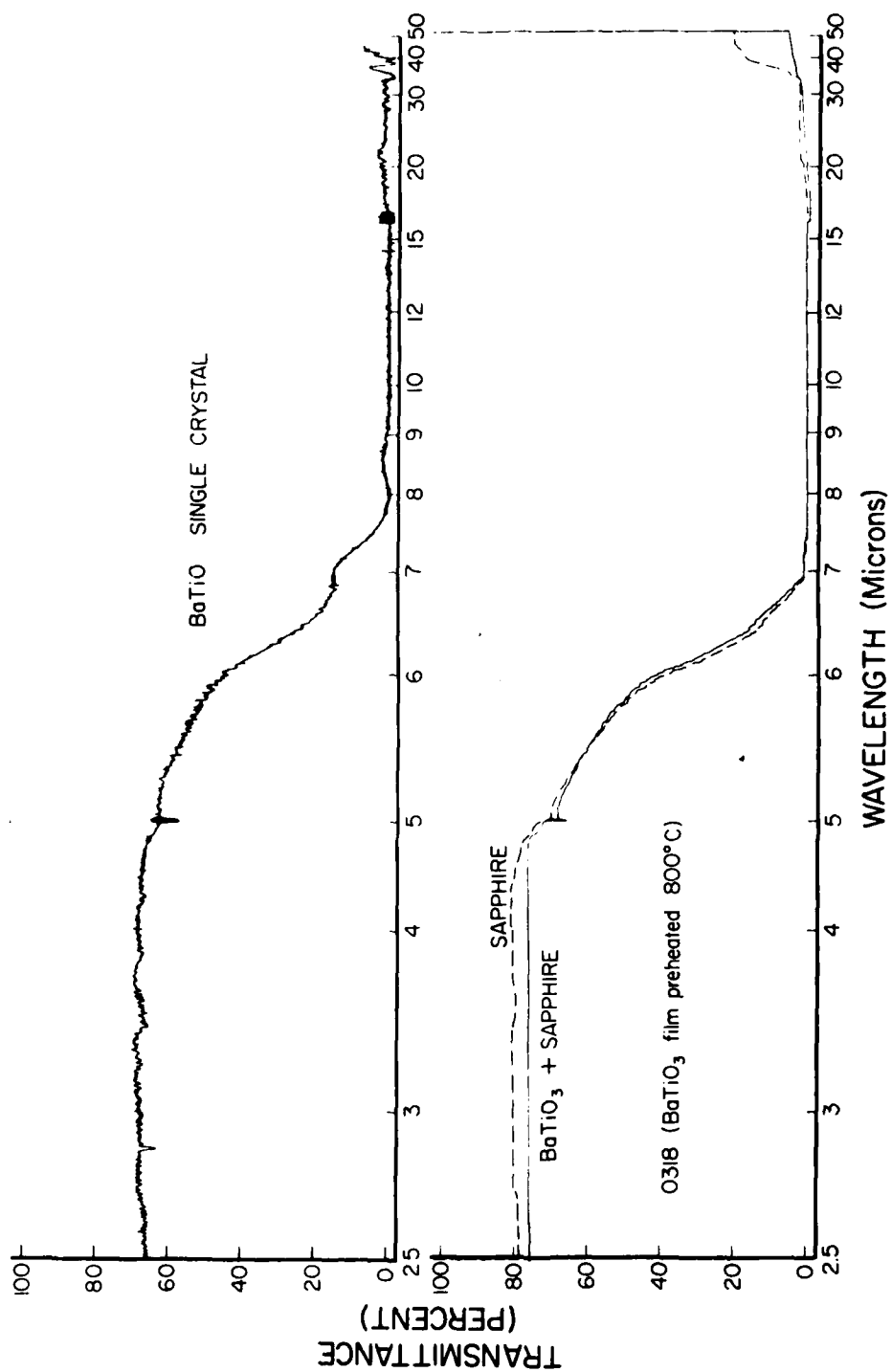


Figure 10. IR Transmission Spectra of a Sapphire Substrate, BaTiO₃ Film and a Single Crystal of BaTiO₃

SECTION III

RESULTS

1. RATE OF BaTiO_3 GROWTH AS A FUNCTION OF THE SPUTTERING POWER

In order to control film thickness, the rate of BaTiO_3 growth (in Å/min) on quartz, sapphire and platinum substrates was determined as a function of sputtering power from 50 to 300 watts in pure argon and in a 5% O_2 /95% Ar mixture (total pressure 15 mTorr). Substrates were preheated to various temperatures: room temperature, 620° C and 800° C. Anode to cathode spacing was 30 mm.

From Figure 11 and Table 1, it appears that the deposition rate is linearly proportional to the sputtering power. The rate decreases about 16-22% with the addition of oxygen. Such a decrease of sputtering yield is expected due to the capturing of secondary electrons by the oxygen. Similar results were reported elsewhere (Reference 6). The substrate temperature does not appreciably affect the yield.* The rate of growth on the platinum substrate is lower than that on sapphire or quartz which might be attributed to enhanced back sputtering from platinum (see Table 1).

2. DIELECTRIC CONSTANTS AND ELECTRICAL CONDUCTIVITY

The room temperature dielectric constants and electrical conductivity of BaTiO_3 films sputtered on platinum foil substrate under various conditions are as shown in Table 2. The data on the dielectric constant in Table 2a are in agreement with the results found for amorphous BaTiO_3 films (Reference 6). The data in Table 2b are in agreement with the results on tetragonal films (Reference 7 and 8). The conductivity of the ceramic pellet was found to be $2.2 \times 10^{-8} \text{ ohm}^{-1}\text{cm}^{-1}$. The low conductivity of the films indicates a low level of impurities, high stoichiometry and very low optical absorption. The problem of electrode

* This result was consistent for preheating up to 602° C (surface temperature 850° C). One run on sapphire preheated to 800° C (surface temperature 1000° C) yielded a rate of 60.1 Å/min.

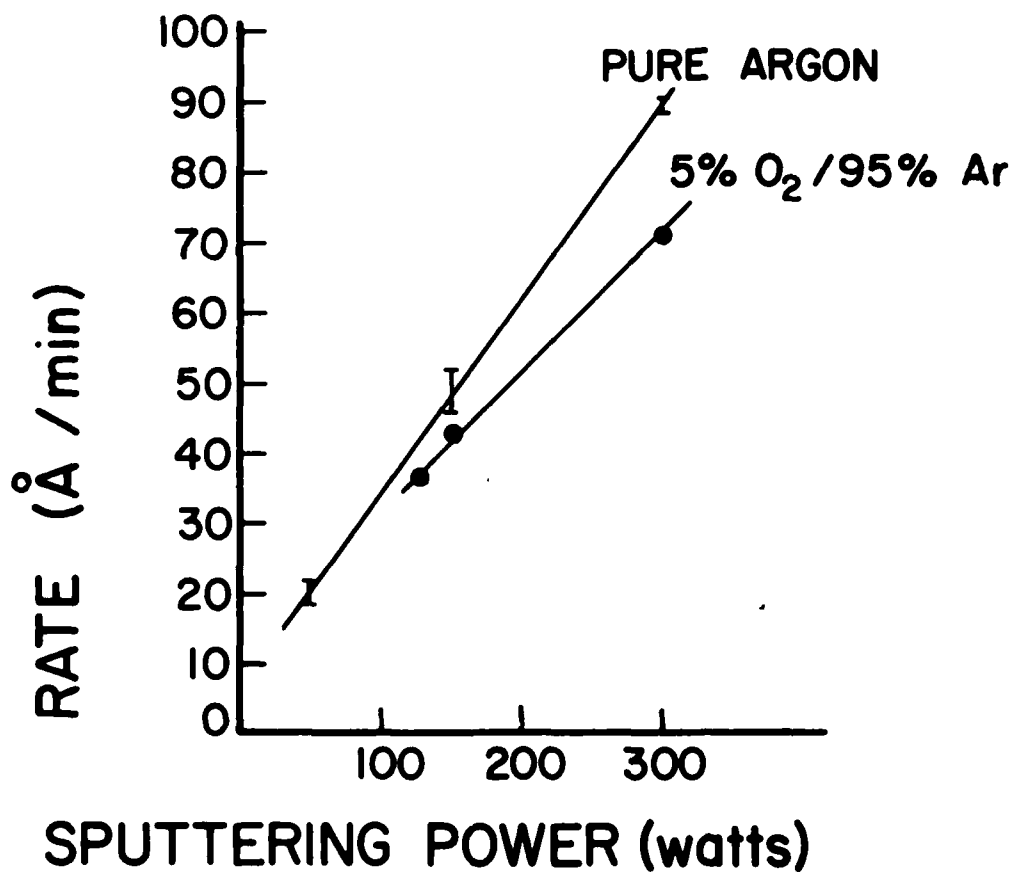


Figure 11. Rate of BaTiO₃ Film Growth as a Function of the Sputtering Power

TABLE 1
DEPOSITION RATES OF SPUTTERED BaTiO₃ FILMS AS A FUNCTION OF SPUTTERING
POWER FOR VARIOUS GAS MIXTURES AND SUBSTRATE TEMPERATURES

Power (Watts)	Deposition Rate on Quartz and Sapphire Total Pressure of gas 15 mTorr (Å/min)		Deposition Rate on Platinum in 5% O ₂ /95% Ar at 620° C** (Å/min)
	Pure Argon Room Temperature*	5% O ₂ /95% Ar 620° C Room Temperature*	
50	19-22		11
125		37	
150	46-52	43	48
300	89-91	71.5	83
			70

*No preheating.

**Preheating to 620° C.

TABLE 2
ELECTRICAL PROPERTIES OF SPUTTERED BaTiO₃ FILMS

a. Films Sputtered in Pure Argon on Substrate Held at Room Temperature. Sputtering Power: 150 Watts.

Film Thickness (Å)	Dielectric Constant (MKS)	Electrical Conductivity (ohm ⁻¹ cm ⁻¹)
28,800 \pm 2000	16	1.4 x 10 ⁻¹⁰
48,000	30	

b. Films Sputtered in 5% O₂/95% Ar on Substrate Preheated to 620° C. Sputtering Power: 150 Watts.

Film Thickness (Å)	Dielectric Constant (MKS)	Electrical Conductivity (ohm ⁻¹ cm ⁻¹)
20,000	160	3.4 x 10 ⁻¹⁰
7,500	210	4.0 x 10 ⁻¹⁰

shorting found in this work and reported by other authors is probably caused by back sputtering of the film by negative oxygen ions (Reference 6). The bombardment by these ions causes pin holes in the film. No improvement of contact shorting was found on reducing the rf voltage from 1000 to 460 volts or by changing the atmosphere from 5% O₂/95% Ar to pure argon, both at a total pressure of 15 mTorr. Therefore, to produce some unshorted metal contact by sputtering, one has to apply many contacts of very small area. In the present work, we successfully used very viscous silver epoxy instead.

3. TRANSMISSION SPECTRA AND ABSORPTION EDGE

In the wavelength range 400 nm - 6.5 μ m, the transmittance of BaTiO₃ films on quartz and sapphire was high and showed no absorption bands. The same behavior was found essentially for the single crystal (see Figure 10). The sharp absorption edge of BaTiO₃ around 250 - 400 nm is caused by direct, allowed band-to-band transitions. For such a transmission absorption edge, the relation of the absorption coefficient, α , to the band gap, E_g , is

$$\alpha^2(h\nu)^2 \sim (h\nu - E_g) \quad (3)$$

where $h\nu$ is the photon energy, and $(h\nu)^2$ is practically constant in the range where Equation 3 is valid (Reference 9).

For amorphous semiconductors, Fritzsche gives a relation (Reference 10)

$$\alpha \sim (h\nu - E_g)^2/h\nu \quad (4)$$

Thus, from these relations, values of E_g can be found by extrapolating to zero the linear portions of either α^2 vs. $h\nu$ or $\sqrt{\alpha h\nu}$ vs. $h\nu$, α^2 vs. $h\nu$ being more appropriate for the bulk material and $\sqrt{\alpha h\nu}$ vs. $h\nu$ for the amorphous thin films. Transmission spectrophotometric

measurements yield the optical density, $OD = -\log T$, where T is the transmittance. Since $T/(1-R) = e^{-\alpha d}$ where R is the reflectance and d is the film thickness, we have

$$\alpha = (d \log e)^{-1} [OD + \log(1-R)] \quad (5)$$

R can be estimated from the relation

$$R_{total} = 2R_F/(1+R_F) \quad (6)$$

where R_F is the Fresnel reflectance $\left[\frac{n-1}{n+1} \right]^2$.

The transmission spectra in the vicinity of absorption edge for various films on sapphire and quartz and that of the single crystal are shown in Figure 12.

Plots of α^2 vs. $h\nu$ calculated from the above data are given in Figure 13. Similarly, in Figure 14 a plot of $\sqrt{\alpha h\nu}$ vs. $h\nu$ is shown. The values of E_g were reasonable as found from the two types of extrapolations.

It is seen from Table 3 that the absorption edge energy gap of $BaTiO_3$ films deposited on non-preheated substrates is independent of the substrate. Since under these conditions amorphous $BaTiO_3$ films are produced, we conclude that the energy gap for such films is 4.12 eV in good agreement with the value of 4.3 eV obtained by Onton and Marrello (Reference 11) and slightly lower than the value 4.6 eV found by McClure and Crowe (Reference 6) for similar films.

In a sputtering atmosphere of 5% O_2 /95% Ar and a substrate surface temperature 650° C, where according to X-ray diffraction, a very small amount of crystallinity is introduced into the films, the absorption edge value of films is 4.10 eV. A decrease of E_g is observed with

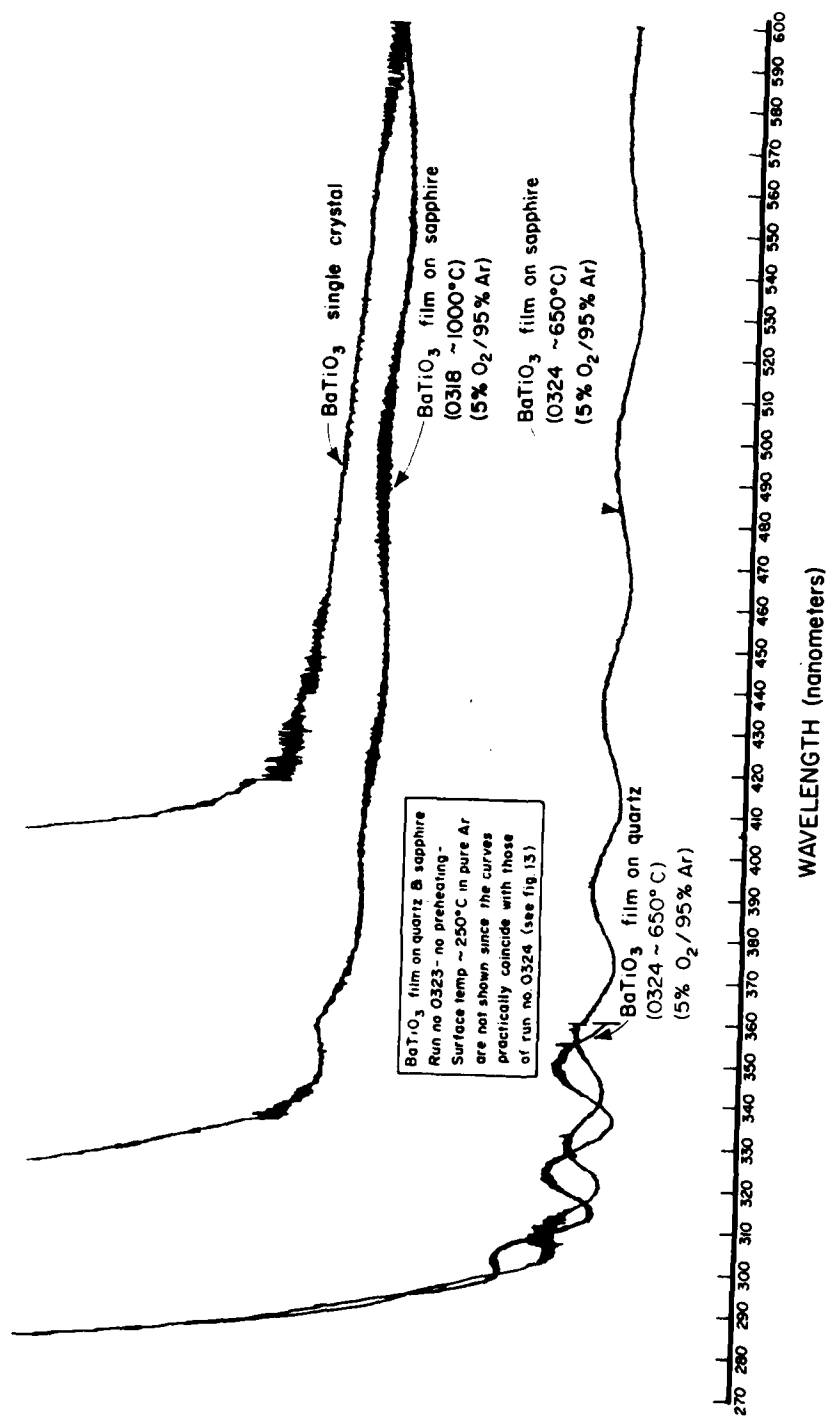


Figure 12. Typical Transmittance in the Vicinity of the Absorption Edge for BaTiO_3 Films and a Single Crystal

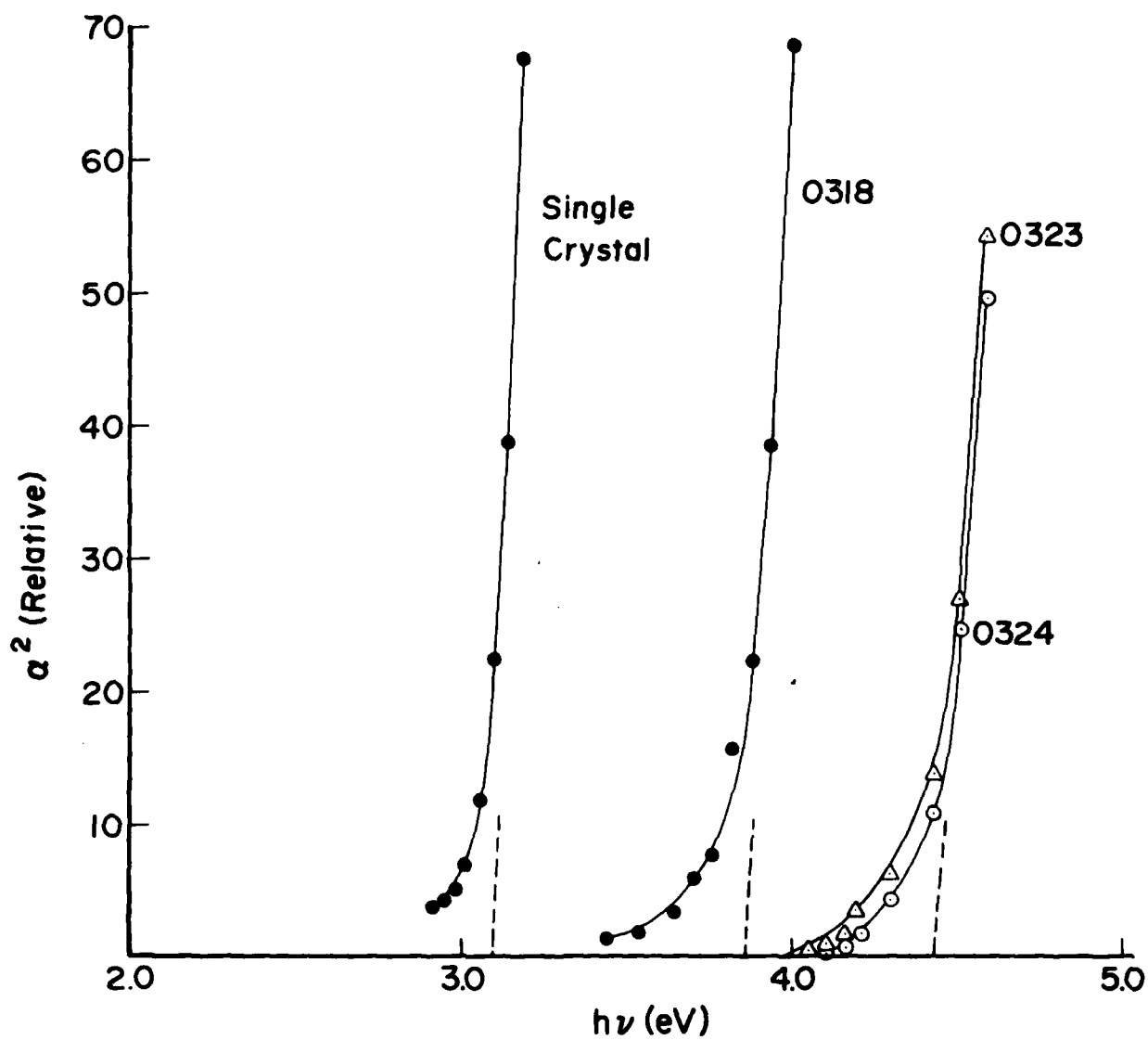


Figure 13. Determination of Band Gap Energy, E_g , from α^2 vs. $h\nu$

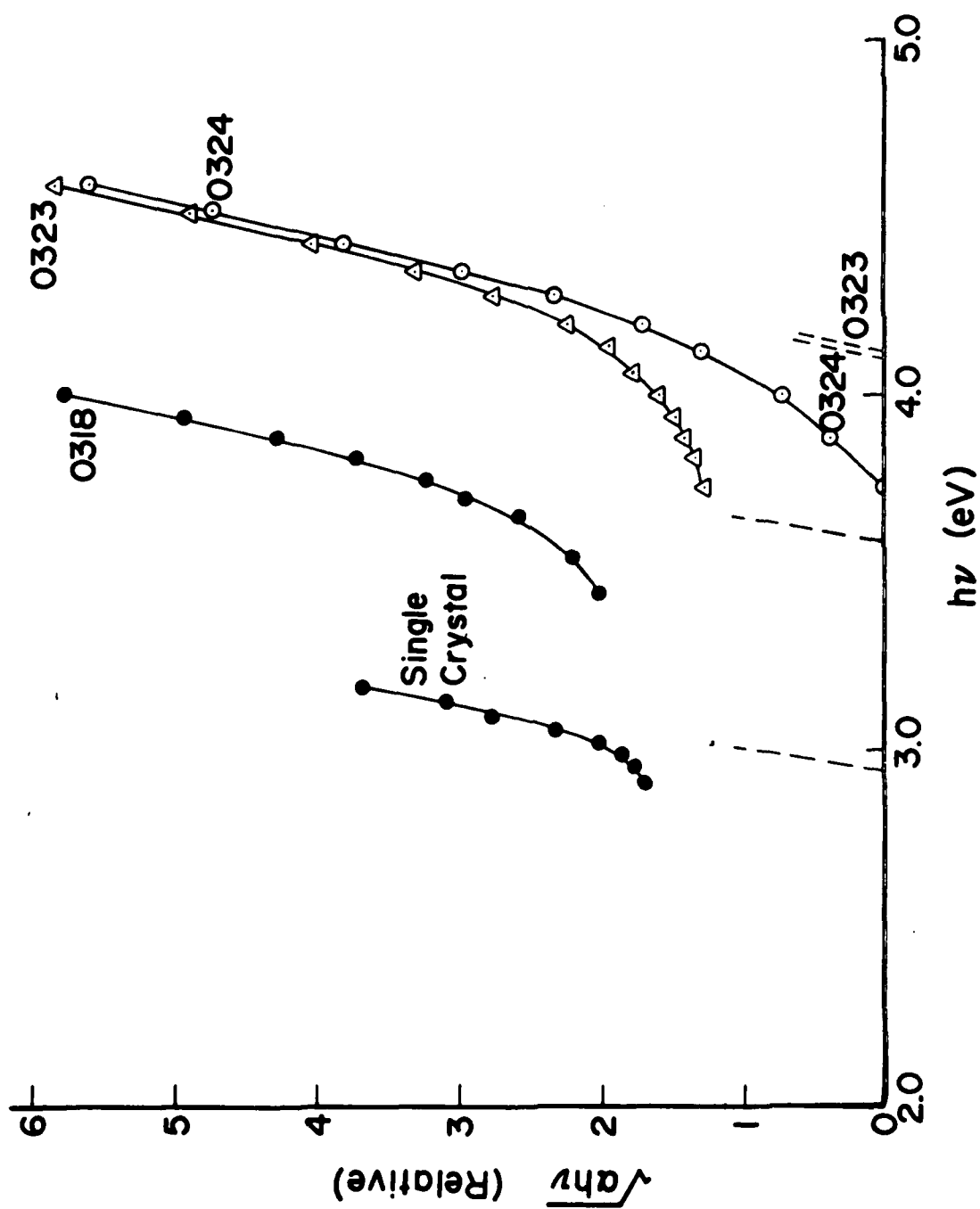


Figure 14. Determination of Band Gap Energy, E_g , from $\sqrt{ah\nu}$ vs. $h\nu$

TABLE 3

ABSORPTION EDGE ENERGY GAP FOR BaTiO_3 FILMS SPUTTERED
UNDER VARIOUS CONDITIONS AND A BaTiO_3 SINGLE CRYSTAL

Run No.	Film Thickness (Å)	Sputtering Conditions	Substrate	E_g (eV)	
				Equation (3)	Equation (4)
	Crystal 1mm			3.10	2.93
0318	4510	800°C preheating at 300 Watts ~1000° C surface temperature 5% O_2 /95% Ar	Sapphire	3.86	3.58
0324	6900	450°C preheating at 200 Watts ~650°C surface temperature 5% O_2 /95% Ar	Sapphire quartz	4.43 4.43	4.10 4.10
0323	5580	No preheating at 200 Watts ~ 300°C surface temperature pure argon	Sapphire quartz	4.43 4.43	4.12 4.12

a further onset of crystallinity in the films, $E_g = 3.58$ eV. The value for a single crystal BaTiO_3 was found to be 3.10 eV. This is lower than the value 3.6 eV previously reported (References 6 and 11).

4. DENSITY MEASUREMENTS

Quartz, sapphire and platinum foils were used as substrates for density determination of BaTiO_3 films. The substrates were weighed before and after the sputtering process by a microbalance. Side edges of the substrate were masked so only the upper substrate surface collected sputtered material. The film thickness was determined by etching a step as previously described. Weight gains were in the range of 1200-7000 μgm for film thickness of 500-30,000 Å.

We found that platinum lost weight during the sputtering process. Quartz and sapphire substrate weights were unchanged during sputtering and etching* within the experimental error of weight measurement ($\pm 10 \mu\text{gm}$). Results on Pt were therefore excluded.

The handbook density of tetragonal crystalline BaTiO_3 is 6.017 gm/cm^3 (5.806 gm/cm^3 for cubic). The apparent density of the high temperature sintered ceramic samples (Reference 1) used in the present work as reference is 5.82 gm/cm^3 , 96.7% of the crystalline material, where the apparent density is defined by the weight of the sample divided by the apparent volume of the sample. From Table 4a it is seen that the value of $4.30 \pm 0.08 \text{ gm/cm}^3$ found for amorphous BaTiO_3 films is only 71.5% of the bulk tetragonal crystalline density. A marked increase of apparent density is found for films with crystalline characteristics as seen in Tables 4b and 4c. The apparent density for films prepared on substrates preheated to 620°C is 4.86 ± 0.15 i.e., 80.1% of the crystalline density and 83.5% of the high density hot pressed polycrystalline material. The higher apparent film density, $5.61 \frac{\text{gm}}{\text{cm}^3}$ (93% of the single crystal) was obtained for 800°C preheating where substrate surface temperature approached 1000°C .

*Quartz lost weight during the etch step; however, the etch step was done after the weight was determined so that the etch step does not affect the apparent density measured.

TABLE 4

APPARENT DENSITY OF BaTiO_3 FILMS SPUTTERED UNDER VARIOUS CONDITIONS
ON QUARTZ AND SAPPHIRE SUBSTRATES IN 15 mTorr TOTAL PRESSURE

a. Films Sputtered in Pure Argon on Substrates at Room Temperature
(Not Preheated)

Run No.	Substrate	Sputtering Power (Watts)	Sputtering Rate ($\text{\AA}/\text{min}$)	Thickness (\AA)	Density (gm/cm^3)
0190	Quartz	160	54	8140	4.33
0192a	Sapphire	300	89	3100	4.35
0197	Quartz	50	20	2780	4.22

b. Films Sputtered in 5% O_2 /95% Ar Mixture on Substrates Preheated
to 620° C

Run No.	Substrate	Sputtering Power (Watts)	Sputtering Rate ($\text{\AA}/\text{min}$)	Thickness (\AA)	Density (gm/cm^3)
0202	Quartz	300	73	7490	4.86
0202	Sapphire	300	70	7220	4.77
0204	Quartz	150	43.5	7925	5.01
0204	Sapphire	150	43	7811	4.79

c. Film Sputtered in 5% O_2 /95% Ar Mixture on Substrate Preheated to
800° C (Surface Temperature ~1000° C)

Run No.	Substrate	Sputtering Power (Watts)	Sputtering Rate ($\text{\AA}/\text{min}$)	Thickness (\AA)	Density (gm/cm^3)
0318	Sapphire	300	60.1	4510	5.61

The apparent density of $4.3 \pm 0.08 \text{ gm/cm}^3$ measured for BaTiO_3 films sputtered at room temperature on substrates in the 5% O_2 /95% Ar mixture indicates that the increase of apparent density is solely due to the substrate temperature. The measurements of the apparent density reveals a high porosity of the amorphous films. If the porosity is defined by

$$V_o/V_{\text{app}} = 1 - \frac{\rho_{\text{app}}}{\rho_x} \quad \text{where } V_o \text{ is the pores volume in the film, } \rho_{\text{app}} \text{ and } V_{\text{app}}$$

the measured density and volume and ρ_x is the X-ray density, then the porosity of the amorphous films is 27% compared to 5% of the highly crystalline films.

5. X-RAY DIFFRACTION

X-ray diffraction intensity vs. diffraction angle was measured for BaTiO_3 films on sapphire, quartz, and platinum. The quartz substrate was excluded since its X-ray line overlapped the BaTiO_3 film line at $2\theta = 21.5^\circ$. X-ray diffraction intensity vs. diffraction angle is presented in Figure 15 for the ceramic pellet and films deposited under various conditions. A least squares computer fit to the diffractive angles yielded the following lattice parameters:

- (1) Ceramic pellet: $a = 3.994 \text{ \AA}$, $c = 4.038 \text{ \AA}$ in agreement with the standard values quoted for bulk BaTiO_3 .
- (2) For 4510 \AA thick films (run 0318) produced on sapphire and platinum at 1000° C surface temperature in 5% O_2 /95% Ar atmosphere.
 - On Pt; $a = 4.04 \text{ \AA}$ and $c = 4.120 \text{ \AA}$
 - On Sapphire; $a = 4.047 \text{ \AA}$ and $c = 4.14 \text{ \AA}$
- (3) For non-preheated film 5580 \AA thick (run 0324) on sapphire, only an estimation could be made since only the $2\theta = 31.0^\circ \pm 1.5$ could be correlated with the reference ceramic sample (see Figure 15). Here $a = c = 4.016 \text{ \AA} \pm 0.06$.
 A film 6900 \AA thick prepared at 450° C , 200 watts, i.e. 650° C surface temperature, in 5% O_2 /95% Ar (run 0323) showed practically the same diffraction pattern as the non-preheated run with only slightly more developed lines (see Figure 15).

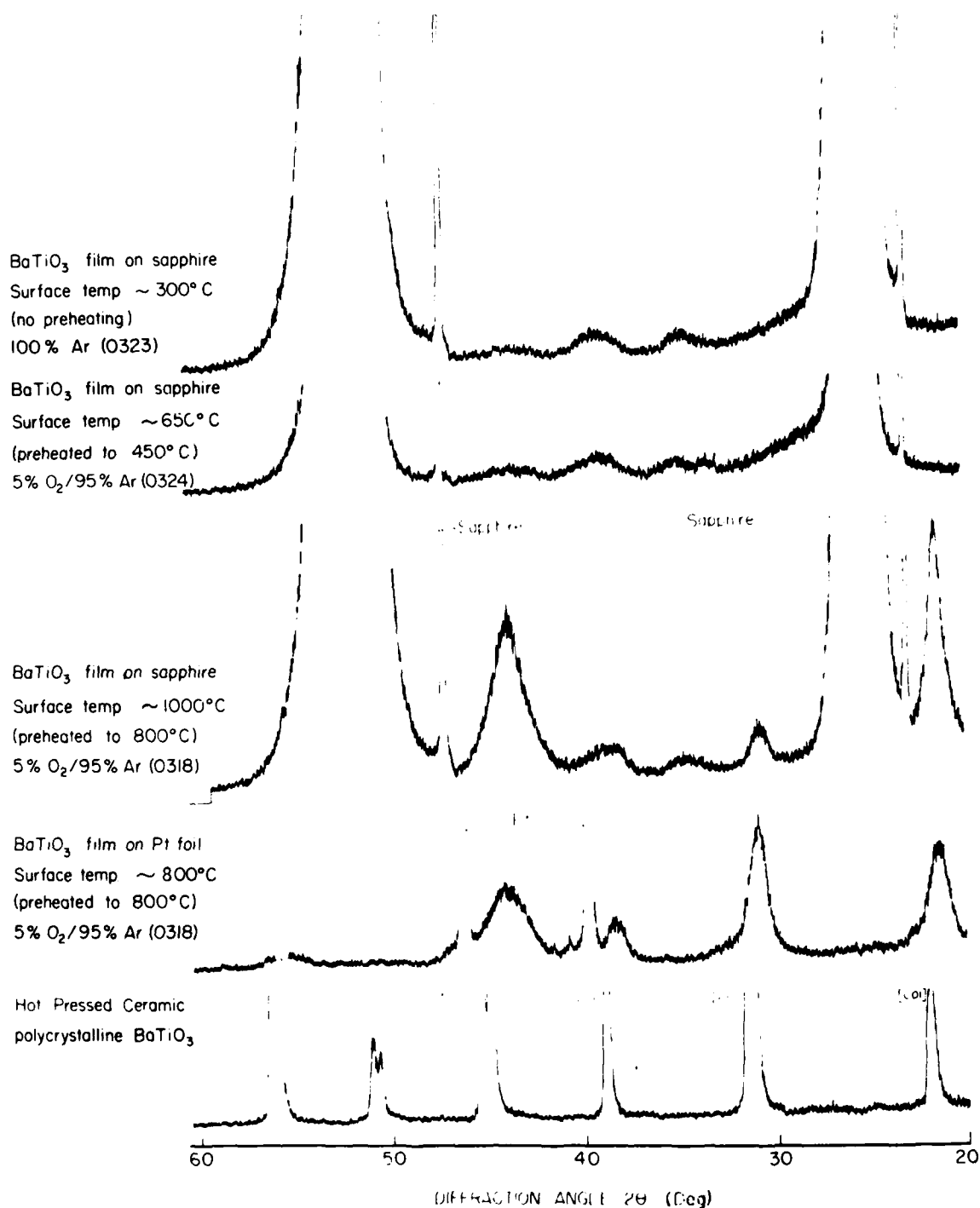


Figure 15. X-ray Diffraction Intensity vs. Diffraction Angle for Films and the Ceramic BaTiO₃ Pellet

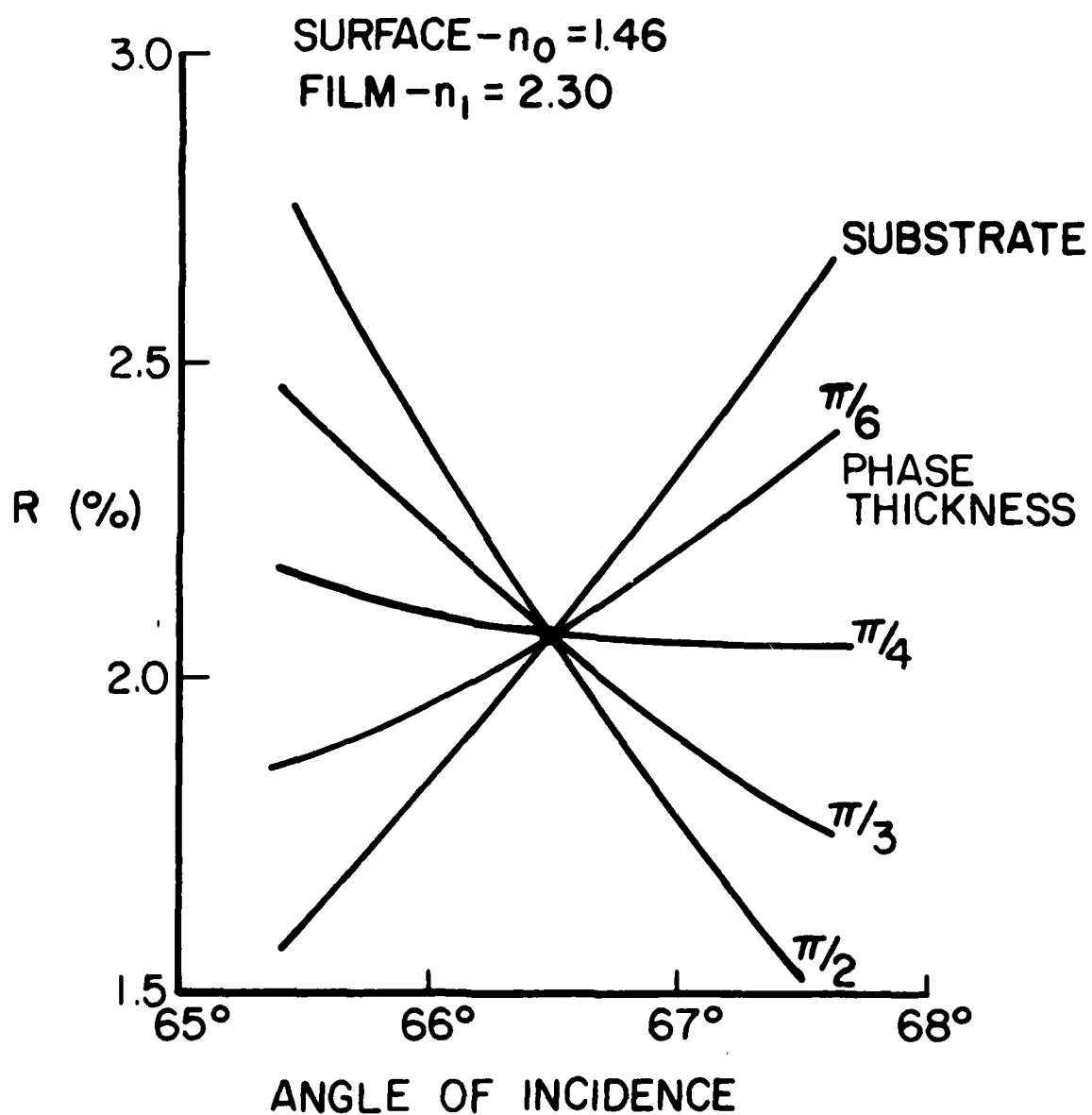


Figure 16. Variation of Reflectivity with Angle of Incidence for Substrates and for Films of Various Thicknesses

This last result proves two important points:

- a. There is a threshold surface temperature above 700° C for growth of tetragonal crystalline BaTiO₃ films.
- b. The crystallinity of the films is due to the temperature and not to the presence of oxygen as can be seen from the results of runs 0323 and 0324 shown in Figure 15.

6. INDEX OF REFRACTION MEASUREMENTS

a. Method of Index Measurements

Preliminary measurements of the refractive index of BaTiO₃ films were made at room temperature using a Gaertner automatic ellipsometer. A value of $n = 1.9$ with He-Ne laser light was found for 1000 Å thick BaTiO₃ film sputtered at room temperature in argon on a Si wafer ($n = 3.6$ and $k = -0.80$ was assumed for Si). This result is in agreement with the value given by Panitz for similar film (Reference 8).

No other reported index measurements of BaTiO₃ films were found in the literature. The above ellipsometer was essentially designed for thickness measurements of thin films on Si substrates ($d \leq 1000$ Å). It was found that for other substrates like sapphire and quartz and film thickness larger than a 1000 Å, the computed results were unreliable. Further ellipsometric measurements were made using a standard Rudolph manual ellipsometer. Results were in agreement with those obtained with the Gaertner ellipsometer. Ellipsometric measurements can provide a complete set of parameters for a thin film (i.e. n , k and thickness) however, these types of measurements are tedious and involve lengthy numerical calculations.

In the present case, the thickness of BaTiO₃ films could be determined satisfactorily by stylus instruments and preliminary spectrophotometric measurements showed that the films are only weakly absorbing. Therefore, the simple and very precise method

of Abeles could be employed to study the refractive index of BaTiO_3 films as a function of wavelength and temperature (Reference 12). By this method, the film index is found from the Brewster angle of the film, θ_B^f , ($n_f = \tan \theta_B^f$). At this angle the reflection of substrate and film are equal for TM polarized flux. In other words, as long as the film is unabsorbing and optically homogeneous, the reflected TM polarized flux at θ_B^f behaves as if the film were not there.*

The absorption of partially crystalline BaTiO_3 films was estimated from spectrophotometric measurements at normal incidence in reflectance and transmittance. For weakly absorbing films,

$$T/(1-R) \approx \exp \left(- \frac{4\pi kd}{\lambda} \right) \quad (7)$$

where T = transmittance, R = reflectance, k = extinction coefficient, d = film thickness, and λ = wavelength (Reference 13).

A sharp absorption edge was found near 350 nm, the exact position depending on film preparation and on the substrate (see Figure 12). For a film of 2340 Å sputtered in 5% O_2 /95% Ar on sapphire preheated to 620° C at 200 watts, the extinction coefficient was calculated at $\lambda = 520$ nm (the middle of the wavelength range for index measurements) from Equation 7 to be $k = 0.011$. The analysis of Abeles for weakly absorbing films shows that for $k = 0.01$ the apparent index will decrease by only 0.5% for films of index 2.3 on a substrate of index 1.5 (Reference 12). Thus, we felt that Abeles method was suitable for BaTiO_3 films in the wavelength range $\lambda > 400$ nm.

The dependence of the reflectance (p-component) on the angle of incidence in the neighborhood of θ_B^f for a nonabsorbing homogenous film

* The back side of the substrate was abraded to eliminate secondary reflections.

is given for various film thicknesses (phase thickness = $2\pi \frac{n_f^d \cos \psi}{\lambda}$) in Figure 16. θ_B^f can be determined by using a goniometric setup at the position of equibrightness (as determined by eye) of the two halves of a beam reflected from the boundary between the coated and uncoated substrate. However, as seen in Figure 16 the sensitivity depends on the optical thickness of the film. The greatest sensitivity is obtained for an odd multiple of quarter wavelength where the phase thickness is $\approx \pi/2$. Sensitivity decreases, also, when n_f differs from n_{sub} by more than about (Reference 13)

$$n_{sub} - 0.3 < n_f < n_{sub} + 0.3$$

For the preceding reasons, an alternative technique was used to determine θ_B^f . A set of reflectance measurements were taken from both the films and bare substrates in a range of a few degrees around θ_B^f . The intersection of the plots of the reflectances vs. angle of incidence yield $\theta_B^f = \arctan n_f/n_0$ (where n_0 is the index of air). Here only the relative reflectances need to be measured. In addition of being independent on the above restrictions, the reflectance plot also provides information on the precision of the measurements. Furthermore, in the present work, the Brewster angle of the substrate was also determined from the minima of the substrate reflectance curves ($n_s = \tan \theta_B^s$) thus providing an additional check on the cleanliness of the substrate surface and the validity of the measurements. The last technique was also used to study the dependence on wavelength and temperature of the refractive index of ceramic and single crystal samples of BaTiO₃.

The precision of this technique depends on the accuracy of measuring the reflectance amplitude and angle. To determine the influence of an error in reflectance measurements on the resulting n_f for actual conditions i.e. 1% ($\pm 0.5\%$) in reflected intensity and $\pm 0.01\%$ in the incident

angle, a computer program calculating the reflectance equations from the bare substrate and film plus substrate was employed for a film phase thickness of $\frac{\pi}{0.89}$. Two substrates having indices of $n = 1.5$ and $n = 1.7$ were chosen to represent quartz and sapphire and a film index of 2.24 represented the BaTiO_3 . The computed results are given in Figures 17 and 18. The error bars indicate experimental error of 1% ($\pm 0.5\%$) in the reflectance measurements. It is found in this case that the index of a BaTiO_3 film on sapphire can be determined within $\pm 0.06\%$, i.e. $\Delta n \approx \pm 0.0013$, and on quartz substrate the error is $\pm 0.08\%$, i.e. $\Delta n \approx \pm 0.002$. For this accuracy, the precision in the incidence angle reading should be within 0.5 minutes of arc. As long as the films are non-absorbing, this method is not affected by the film thickness and can be used for very thin films. This is in contrast to the less accurate method ($\sim 1\%$) suitable for thick films (above $1\mu\text{m}$) by which the index is determined from the wavelength position of the interference maxima of the transmission spectra.

The determination of the index from the minimum reflectance at the Brewster angle* was, however, less sensitive. For the best resolution of the reflected intensity at the minimum of $\Delta\theta_B \approx \pm \frac{1}{8}^\circ$. The error introduced for sapphire substrates was $\pm 0.5\%$ of the index. The error introduced for the ceramic BaTiO_3 was $\pm 0.6\%$, i.e. $\Delta n \approx \pm 0.015$.

b. Optical System for Index Measurements

A standard manual ellipsometer manufactured by Rudolph Research (type 43603-200E) was modified to allow index measurements to be made by Abeles method. This instrument provides the following features: a well-collimated beam, turning arm positional accuracy of 0.01 degree of arc, Nicol prism polarizers and general ease of handling. Since in the neighborhood of the Brewster angle, the reflected intensity is very low, we desired a high intensity source. We used a xenon arc lamp and a 3 mw He-Ne laser. The high intensity of the xenon source enabled us to

*Used to determine the index of the substrates and that of a ceramic pellet and single crystal.

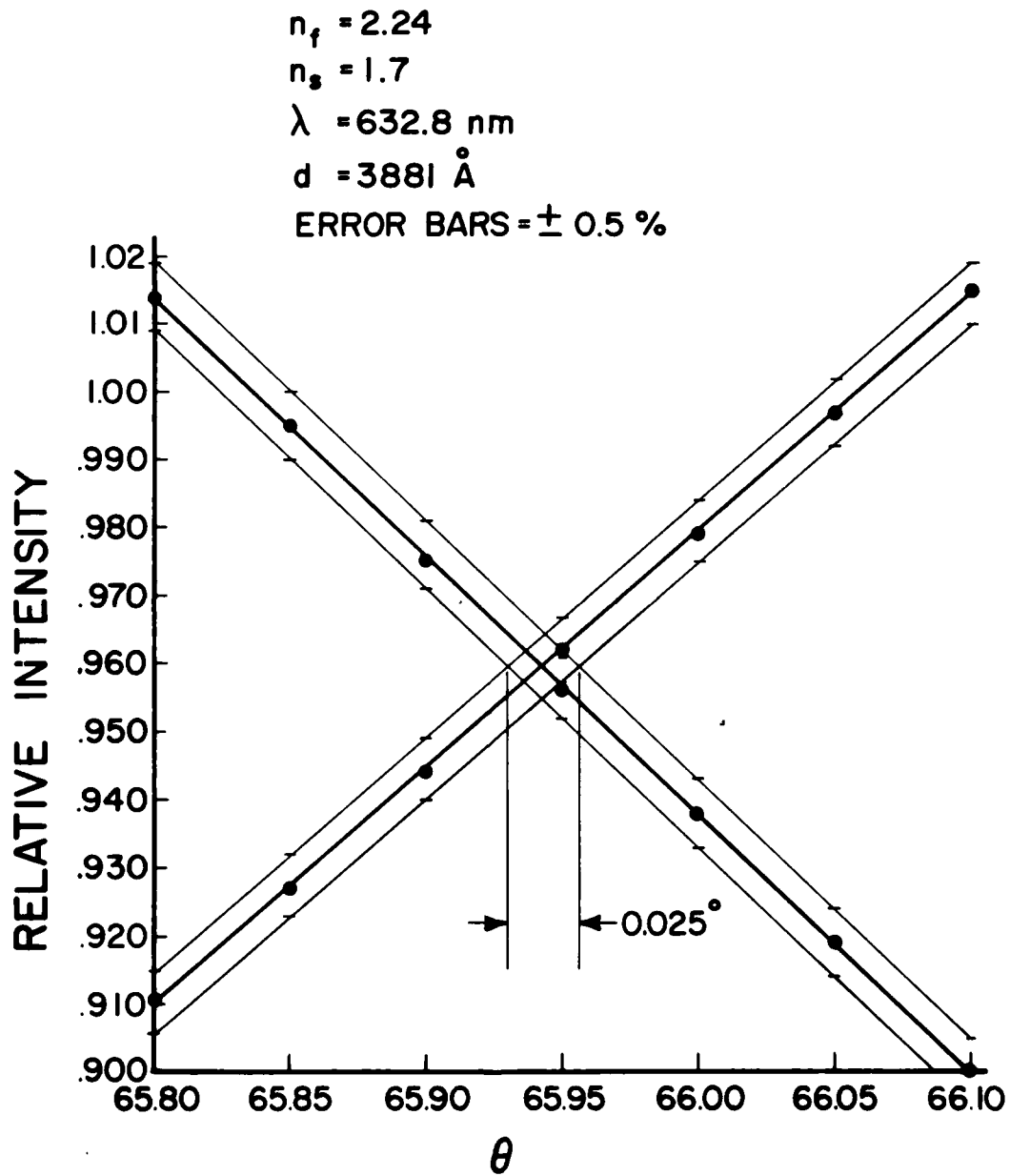


Figure 17. Computed Relative Reflectivity vs. Incidence Angle for a Film on a Substrate with Index of 1.7

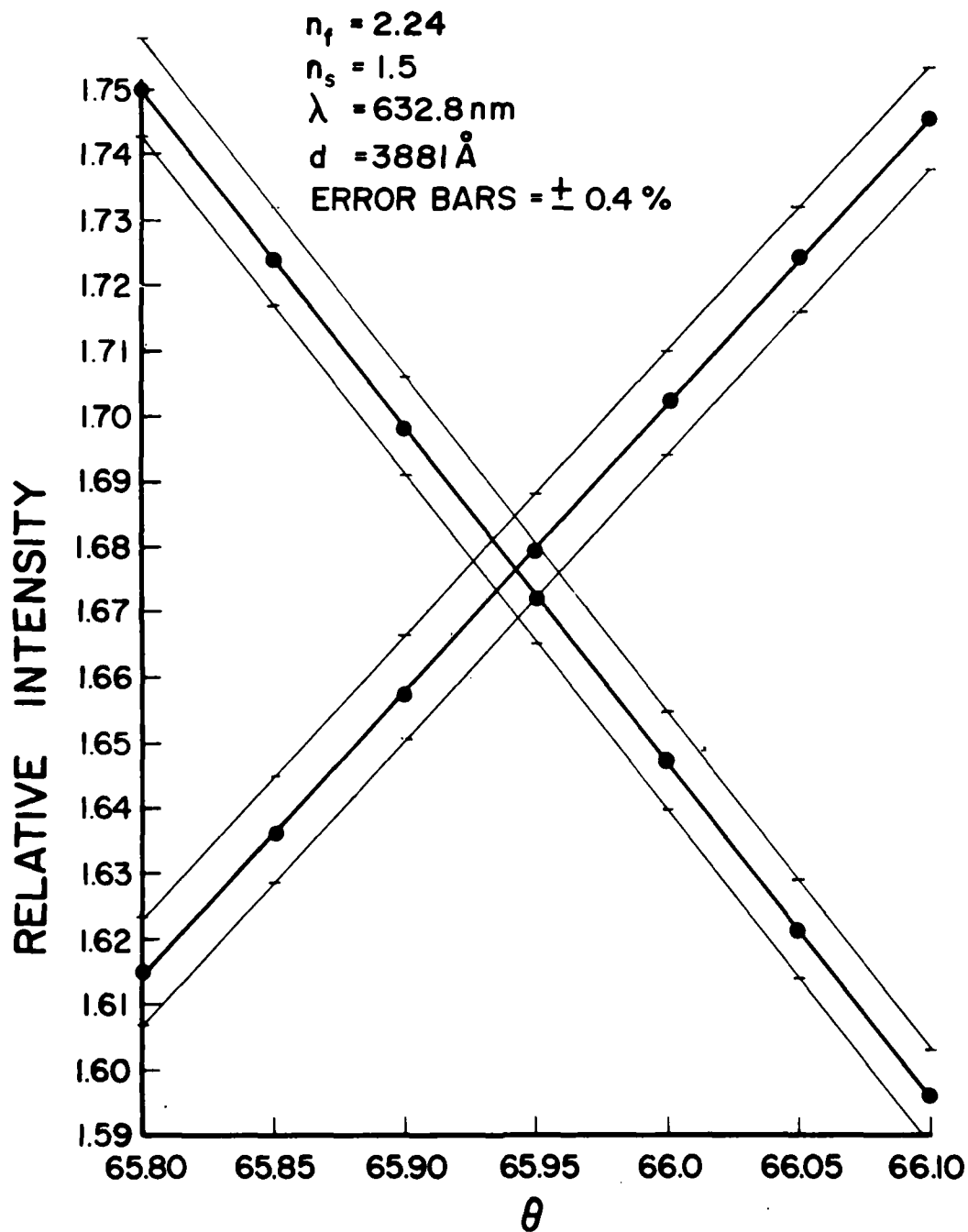


Figure 18. Computed Relative Reflectivity vs. Incidence Angle for a Film on a Substrate with Index of 1.5

utilize a series of narrow-band bypass filters to measure the dispersion from 400 to 600 nm. The He-Ne laser provided the $\lambda = 632.8$ nm.

To cover this spectral range, we used the original RCA IP21 photo-multiplier tube.* To facilitate the setting of the incident angle (as measured by the maximum signal of the PMT) a fine worm-driven rotational table was added to the sample stage. The sample mount has, additionally, x, y, z, and tilt controls. The z control provides reflections from the bare substrate and/or the film at the same angle. The sample is mounted on an aluminum block containing a heater which can be heated to $\sim 300^\circ$ C.

c. Results of Refractive Index Measurements

The refractive indexes of BaTiO_3 films, the ceramic and single crystal samples are given in Tables 5 to 10 as a function of the wavelength in the range 400-632.8 nm at room temperature. Figure 19 summarizes the dispersion data on bulk and thin films of BaTiO_3 . This data is in general agreement with the index measurements of Wohlecke et al., on thick (1-5 μm) rf sputtered BaTiO_3 films derived from the wavelength position of the interference maxima in the transmission spectra (Reference 16). However, in that study the highly crystalline state was not achieved due to the low substrate temperature 30°C and 130°C . Thus, the values of the indexes of the "micro-crystalline" state were 13-14% below the single crystal values as compared to 4.5% of the highly crystalline films in the present study. The index of the films was measured by Abeles method and that of the ceramic pellet and single crystal determined from the minima of the relative reflectivity vs. incidence angle. In the last case, a regression parabolic fit was used to determine θ_B for broad curves, for example at 404 nm in Figure 20. Figure 20 demonstrates how θ_B was determined for the ceramic sample at two wavelengths. Figures 21 and 22 show the relative reflectivity vs. incidence angle at two wavelengths for which the Brewster angle of sapphire and its index were also determined. Figures 23 and 24 show how the index of the films was determined for a narrow range around the intersection.

* An RCA 4832 PMT will directly replace the original IP21 tube of limited response and will enable, in future work, extension of the spectral range to 900 nm.

AFWAL-TR-81-4049

The index of BaTiO_3 films on a preheated substrate and the ceramic pellet is given as a function of temperature in Table 11 and in Figures 25 and 26. Here a xenon lamp was used without filters.

TABLE 5

REFRACTIVE INDEX OF BaTiO_3 SINGLE CRYSTAL
IN THE SPECTRAL RANGE 400-590 NM

Wavelength (nm)	Brewster Angle (degree of Arc)	Refractive Index
404	68.20	2.500
423	67.76	2.446
436	67.70	2.438
486	67.30	2.390
520	67.10	2.367
589	66.93	2.345

TABLE 6

REFRACTIVE INDEX OF BaTiO_3 HOT PRESSED CERAMIC
PELLET IN THE SPECTRAL RANGE 404 - 632.8 NM

Wavelength (nm)	Brewster Angle (degree of Arc)	Refractive Index
404	68.0 ± 0.12	2.475 ± 0.015
450	67.75	2.44
500	67.00	2.35
550	66.60	2.31
589	66.50	2.30
632.8 (He-Ne laser)	66.35	2.28

TABLE 7

REFRACTIVE INDEX OF BaTiO_3 FILM 5320 Å THICK, SPUTTERED
AT 300 WATTS ON SAPPHIRE PREHEATED TO 620° C IN 5%
 O_2 /95% Ar (15 mTorr)

Wavelength (nm)	Brewster Angle (degree of Arc)	Refractive Index
404	66.90 ± 0.02	2.344 ± 0.002
423	66.24	2.272
436	65.45	2.190
450	64.25	2.073
486	66.15	2.262
520	66.00	2.246
589	65.06	2.156

TABLE 8

REFRACTIVE INDEX OF BaTiO_3 FILM 4800 Å THICK, SPUTTERED
 AT 100 WATTS ON SAPPHIRE PREHEATED TO 580° C in 5% O_2 /95%
 Ar (15 mTorr)

Wavelength (nm)	Brewster Angle (Degree of Arc)	Refractive Index
404	65.08 ± 0.02	2.152 ± 0.002
405	64.62	2.108
423	64.12	2.061
436	63.57	2.012
450	62.47	1.918
486	63.58	2.013
500	64.42	2.089
520	64.90	2.135
550	64.80	2.125
589	64.68	2.114
600	64.25	2.073
632.8	63.85	2.036

TABLE 9

REFRACTIVE INDEX OF AMORPHOUS BaTiO_3 FILM, 4550 Å THICK,
SPUTTERED AT 300 WATTS ON SAPPHIRE NOT PREHEATED IN PURE
ARGON (15 mTorr)

Wavelength (nm)	Brewster Angle (Degree of Arc)	Refractive Index
404	63.31 \pm 0.03	1.989 \pm 0.003
450	62.85	1.950
550	62.81	1.947
632.8	62.43	1.915

TABLE 10

TEMPERATURE DEPENDENCE OF THE REFRACTIVE INDEX OF A BaTiO_3
CERAMIC PELLET USING A XENON LIGHT SOURCE

θ_B^f Brewster Angle	n Refractive Index	T Temperature ($^{\circ}\text{C}$)
67.10 ± 0.1	2.367 ± 0.012	20
67.15	2.373	50
67.15	2.373	80
67.32	2.393	120
67.35	2.396	127
67.15	2.373	150

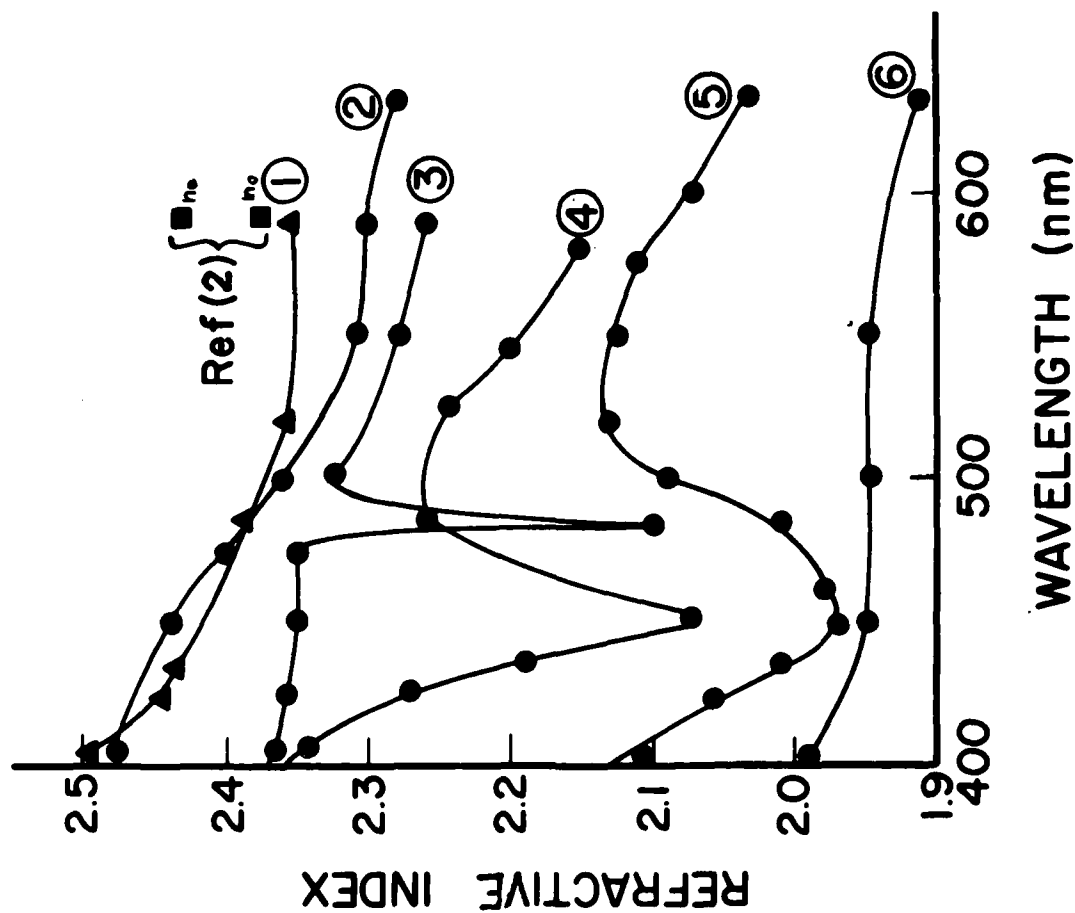


Figure 19. Refractive Index of BaTiO₃ Films, Ceramic Pellet, and Single Crystal vs. Wavelength at Room Temperature

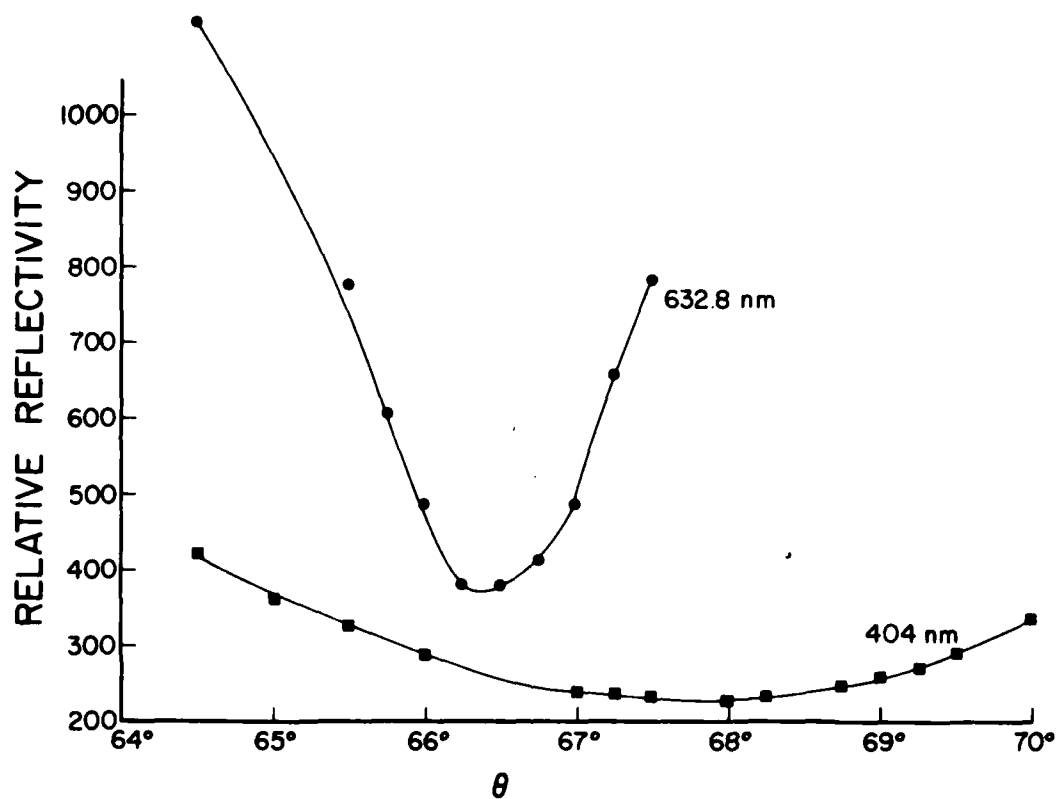


Figure 20. Relative Reflectivity vs. Incidence Angle of BaTiO₃ Ceramic Pellet at 404 nm and 632.8 nm

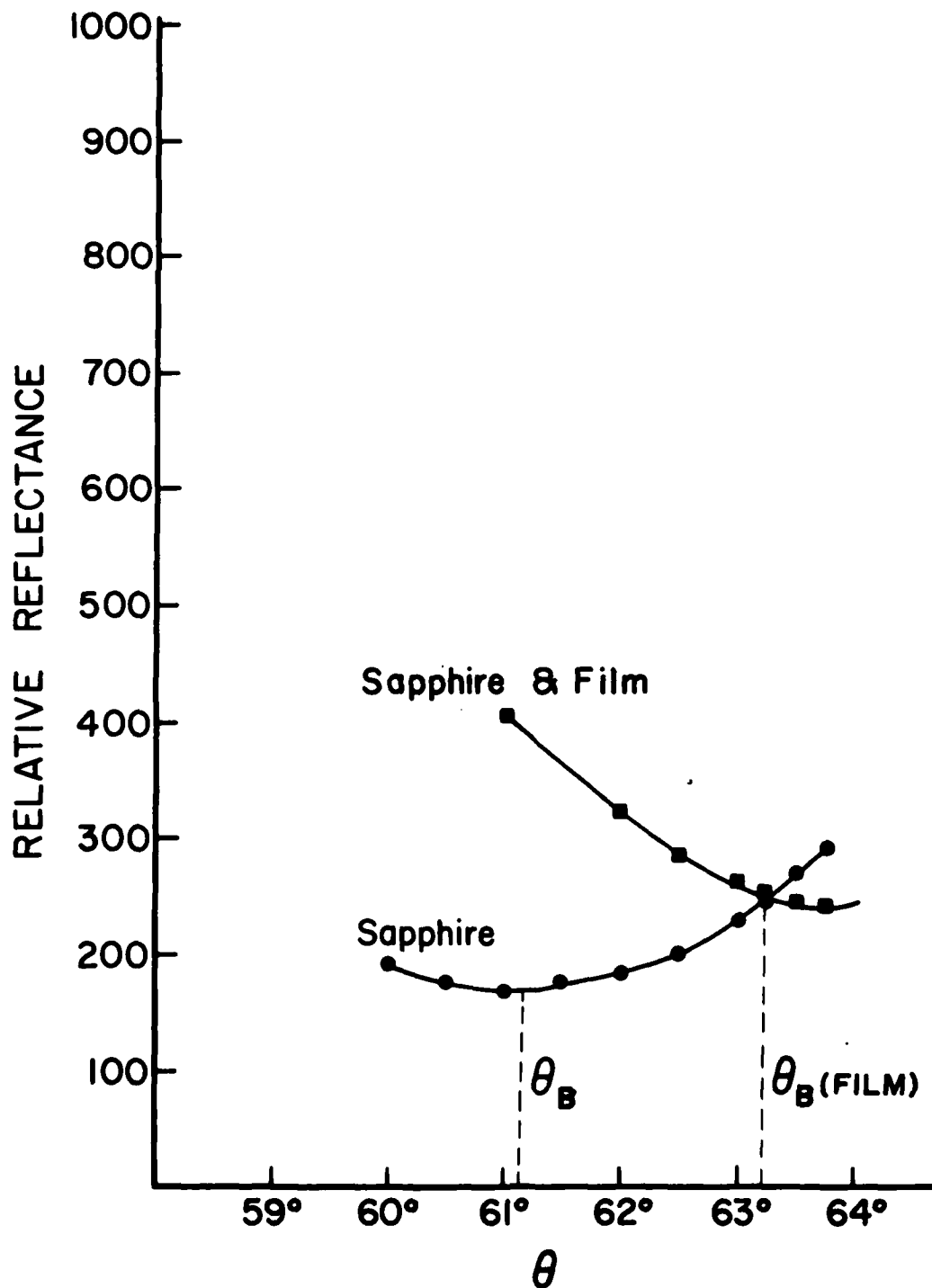


Figure 21. Relative Reflectivity vs. Incidence Angle of an Amorphous BaTiO_3 Film on Sapphire at 404 nm

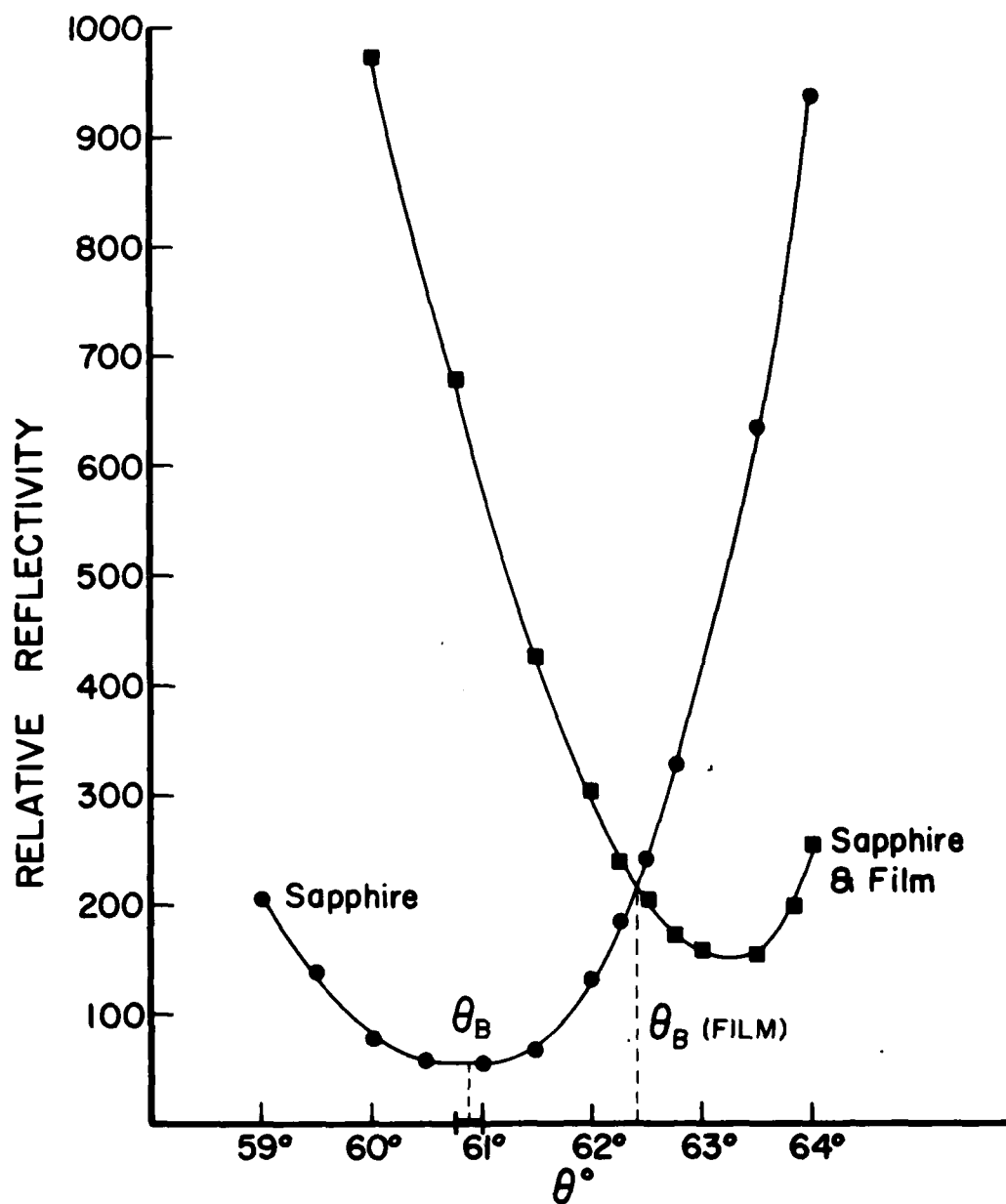


Figure 22. Relative Reflectivity vs. Incidence Angle of an Amorphous BaTiO_3 Film on Sapphire at 632.8 nm

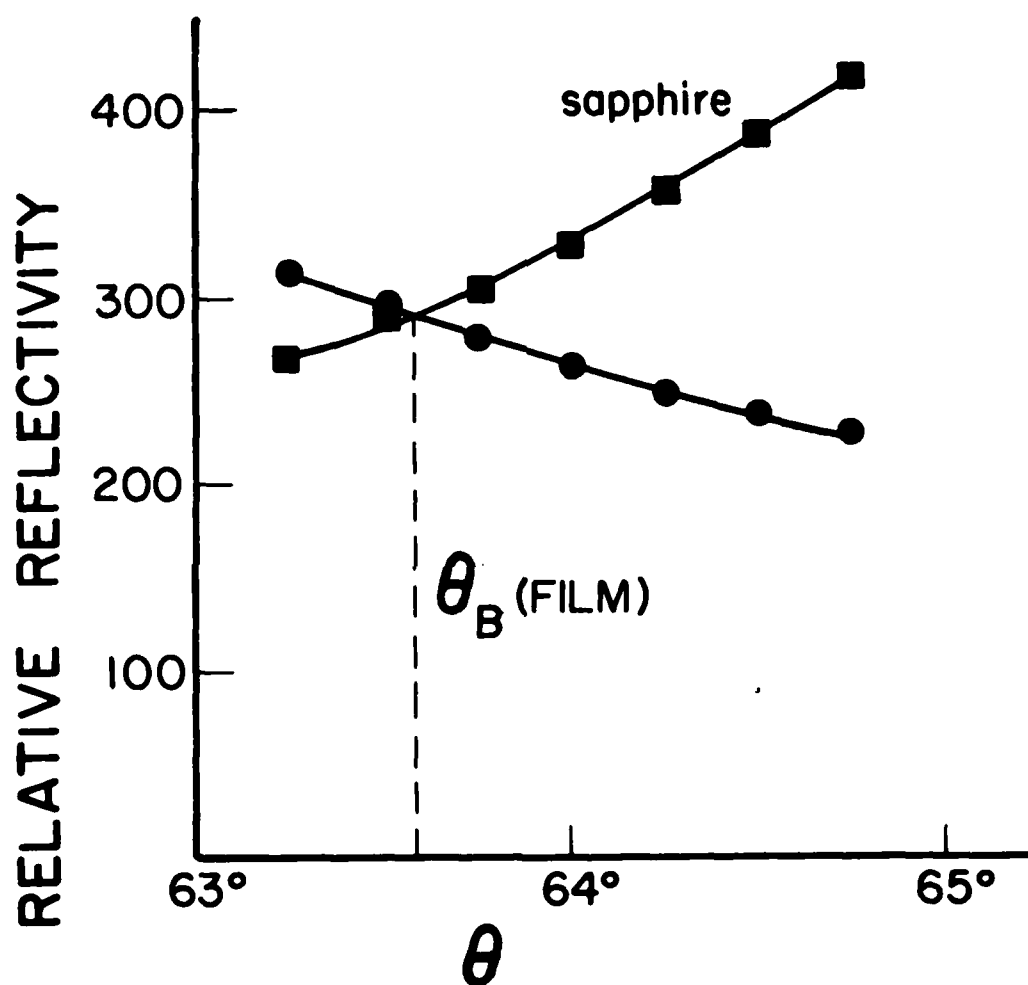


Figure 23. Relative Reflectivity vs. Incidence Angle of an Amorphous BaTiO_3 Film on Sapphire at 436 nm

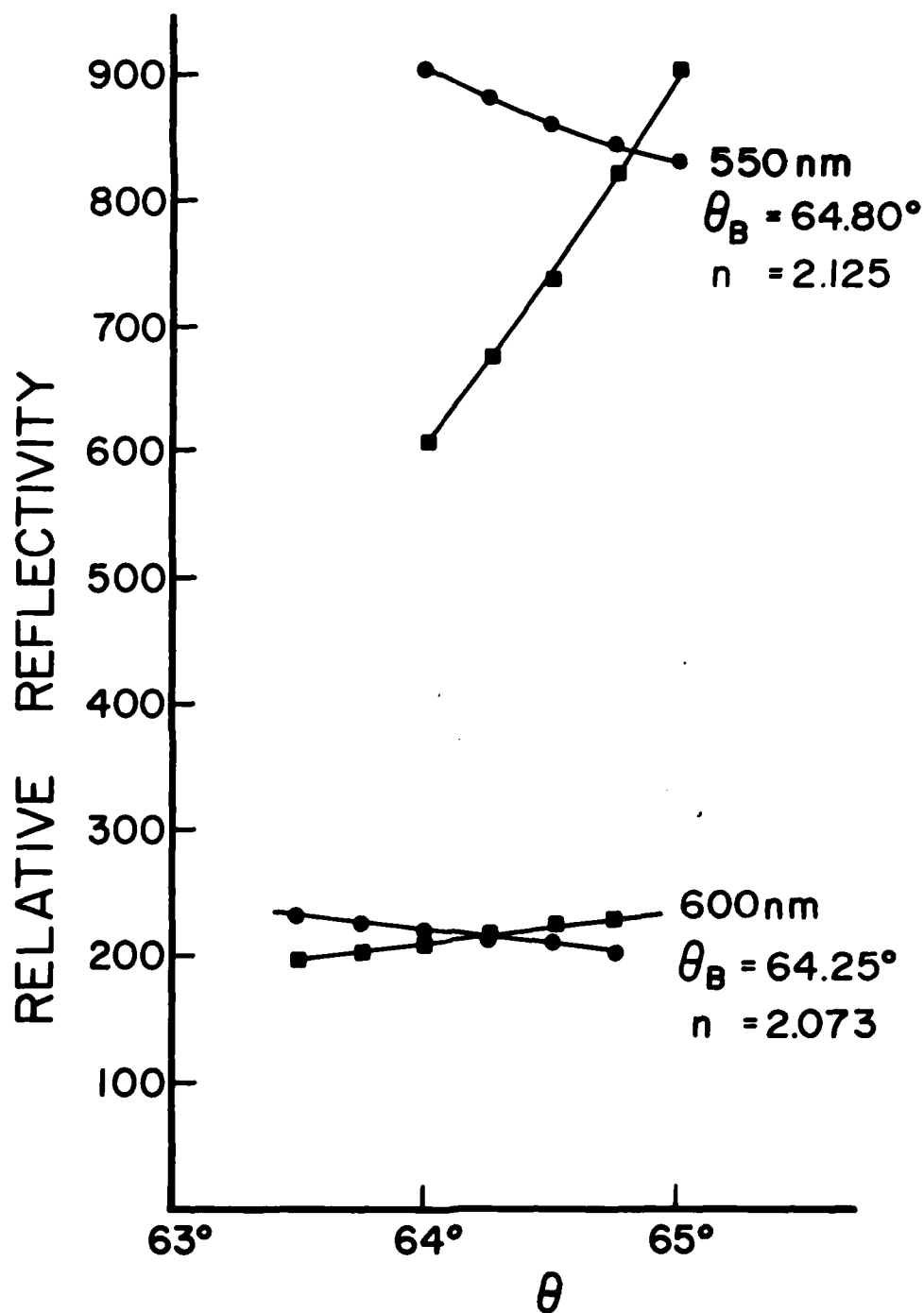


Figure 24. Relative Reflectivity vs. Incidence Angle of BaTiO₃ Film on Sapphire Sputtered at ~800°C Surface Temperature at Two Wavelengths

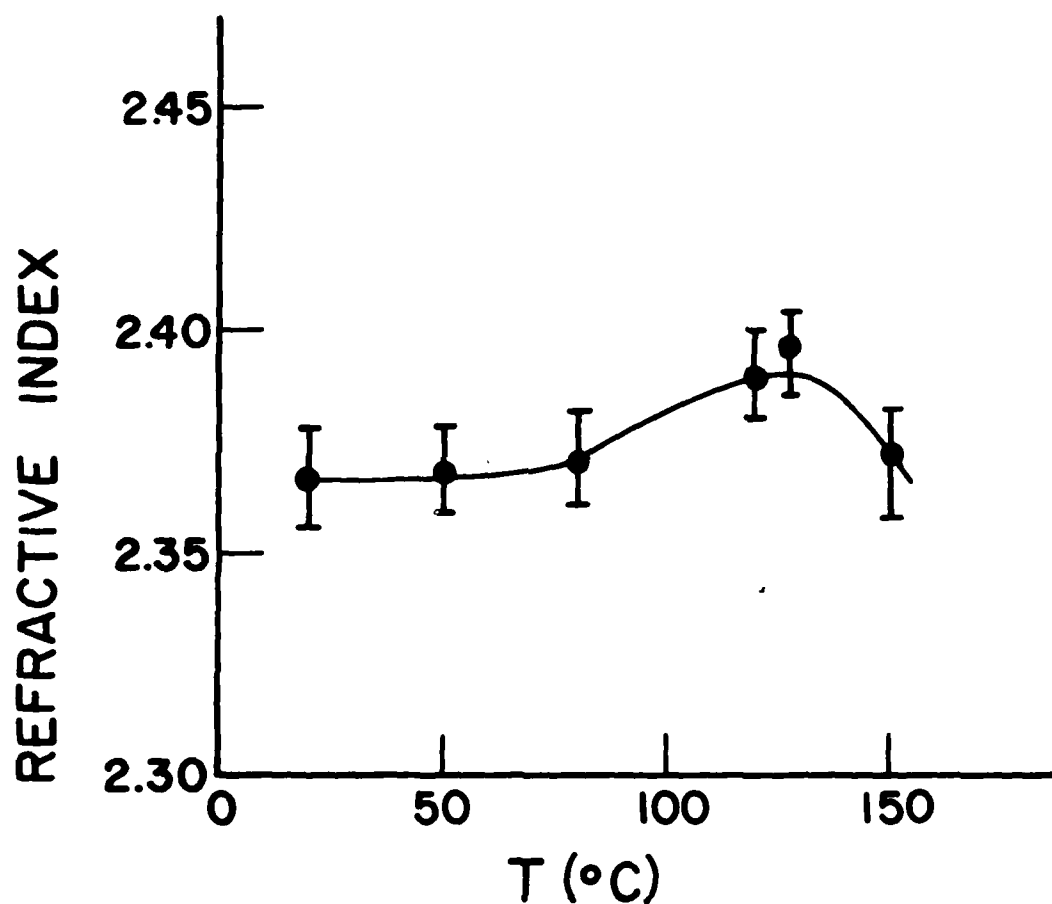


Figure 25. Temperature Dependence of Average Refractive Index of a BaTiO₃ Ceramic Pellet (Xenon Light Source, No Filter)

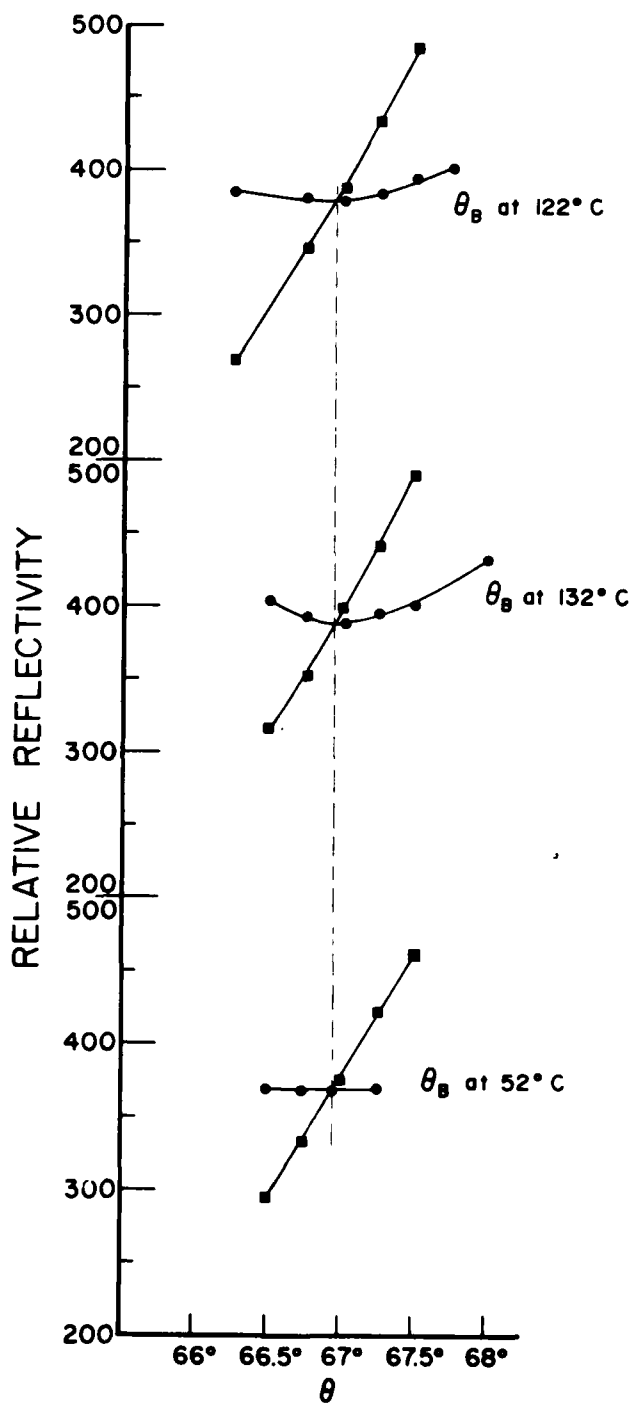


Figure 26. Relative Reflectivity vs. Incidence Angle of a BaTiO_3 Film on Sapphire Sputtered at $\sim 1000^\circ\text{C}$ Surface Temperature

SECTION IV

SUMMARY AND CONCLUSION

Synthesis

1. BaTiO₃ films of uniform thickness (up to ~10 μm) and with reproducible composition can be produced by rf sputtering (Figure 3).
2. Films are transparent and look flawless in SEM up to 20 K magnification. Films formed in argon on unpreheated substrates are colorless. Films on preheated substrates formed in oxygen/argon mixtures appear yellow.
3. Evidences were found for back sputtering which caused pores in the films, both in argon and in the oxygen/argon mixture.
4. Pore sizes were estimated to be less than 1000 Å.
5. Pores caused contact shorting in films sputtered on conductive substrates. Shorting was found for both sputtered and evaporated contacts and could be readily overcome using a viscous conductive paint. It is possible that back-sputtering effects can be reduced with increasing the total pressure (from 15 mTorr to ~100 mTorr).
6. Back sputtering was found to be enhanced on the platinum substrates.
7. The rate of film growth is proportional to the sputtering power (Figure 11).
8. The rate of growth in the oxygen/argon mixture is lower than that in pure argon due to capturing of secondary electrons by the oxygen. In the present study, the rate of growth in 5% O₂/95% Ar was found to be 20% lower than that in pure argon.
9. The upper surface temperature of poor heat conducting substrates like quartz, glass, and sapphire increases rapidly with the sputtering power.

10. Equilibrium surface temperature is reached after ~10 minutes of sputtering.
11. An increase of surface temperatures up to 300° C above the preheating temperature was measured for sputtering powers of 300 watts (Figure 7). Substrates could be preheated to 800° C.

Characterizations

1. Physical properties of BaTiO₃ films differ greatly whether they are deposited on substrates having surface temperatures above or below ~700° C. Films formed at surface temperatures below 700° C manifest X-ray diffraction patterns of amorphous characteristics while those formed above that temperature exhibit partially and strong crystalline characteristics as compared to crystalline diffraction patterns (Figure 15). The apparent density measurements indicate a 27% porosity for the amorphous films compared with only 5% porosity of the highly crystalline films. The transition from amorphous to high crystallinity happens rather abruptly as can be seen from the X-ray and spectrophotometric absorption edge data.
2. No evidences of anisotropy of the crystalline film on sapphire were found in the X-ray diffraction or in polarized flux spectrophotometry. The film crystallinity as appears from X-ray diffraction (Figure 15) and spectrophotometric data (Figure 12) does not depend on the substrate crystallinity as the same results are found on sapphire, quartz, and platinum, nor does it depend on the presence of oxygen in the argon atmosphere.
3. The following table summarizes physical constants of sputtered films in relation to bulk polycrystalline and single crystal BaTiO₃.
4. The high electrical resistivity indicates high material purity, high stoichiometry and low optical absorption.

TABLE 11
SUMMARY OF EXPERIMENTAL DATA ON BaTiO_3 FILMS AND BULK

Material Form	Apparent Density (gm/cm ³)	Lattice Parameter (Å)	Dielectric Constant (room temp)	Electrical Conductivity (ohm ⁻¹)	Energy Gap From Absorption Edge (eV) Eq. 1 Cryst. Eq. 2 Amorp.	Refractive index ($\lambda = 404 \text{ nm}$) (room temp)
Amorphous films	4.30	$a \sim 4.01 \pm 0.06$	20	1.4×10^{-10}	4.43	1.996
Partially crystalline films, (surface temperature $\sim 700^\circ\text{C}$)	4.86	$a \approx c = 4.05$	200	4.0×10^{-10}	4.43	2.344
Highly crystalline films, (surface temperature $\sim 1000^\circ\text{C}$)	5.61	$a = 4.047$ $c = 4.140$	350 - 500**		3.86	2.400
Polycrystalline ceramic	5.82	$a = 3.994$	2000	2.2×10^{-8}		2.475
Single crystal	6.017*	$a = 3.994^*$ $c = 4.038$	$\epsilon_a = 200^*$ $\epsilon_c = 4000$		3.10	$n_c = 2.500$

* Handbook values

** Only an estimate was possible due to shorting of contacts
(Also experienced by Pratt Reference 7)

5. BaTiO₃ sputtered films are weakly absorbing in the spectral range 350-650 nm with an extinction coefficient of approximately $k = 0.01$ at $\lambda = 520$ nm.
6. A sharp absorption edge is found in the spectral range 250-400 nm which depends on the preparation conditions.
7. Precise measurements of the films' refractive index are readily made by Abeles method using a suitably modified standard ellipsometer. The proper combination of light source and detector yield an accuracy of 0.06% for index measurements in the spectral range $400 \leq \lambda \leq 632.8$ nm.
8. The refractive index of the ceramic polycrystalline, partially and highly crystalline films shows strong dispersion in the visible.
9. The dispersion curves of partially crystalline films, measured by Abeles method, exhibit an anomalous dip around 450 nm. No explanation can be provided since no absorption band was found in this particular wavelength region. The more crystalline the film, the narrower is the dip.
10. The capability of producing BaTiO₃ films of large variation in the refractive index, from 1.9 to 2.4, depending on the sputtering conditions, is attractive for multilayered dielectric stacks.
11. The ceramic BaTiO₃ sample shows a slight increase ($\sim 1\%$) of the refractive index at the Curie temperature, 120° C (Figure 25). This behavior relates to the large (4.5 times) increase of the dielectric constant at that temperature (See Figure 9).
12. No temperature dependence of the index was found for crystalline films in the temperature range 15-150° C (See Figure 26). This result is also in accordance with the weak temperature variation of the dielectric constant reported for similar films. The absence of ferroelectric behavior of the crystalline films may be attributed to strong clamping of the films to the substrate as suggested by Verne (Reference 17).

13. It appears that the DC dielectric constant is a most sensitive property for indicating a change of the index caused by external stimulations like temperature, electrical field, stresses, etc. in ferroelectric materials.
14. Preliminary experiments showed no effect on the index from an external electrical field up to 1500 volts either parallel or perpendicular to a partially crystalline film.
15. All the techniques developed in this investigation of BaTiO_3 are equally applicable to the study of other sputtered films and constitute a viable method for screening materials for usefulness as candidates for laser hardened optical systems.

SECTION V

SUGGESTIONS FOR FURTHER WORK

1. The spectral range for index measurements should be extended to ~900 nm by employing an RCA 4832 photomultiplier tube.
2. Photoelectric effects in BaTiO_3 should be investigated. It is suggested to start first with the single crystal to establish an upper limit of any such effects. If results are positive, try highly crystalline sputtered films.

It is suggested to look for changes of index under the influence of electric fields either parallel or perpendicular to the film or crystal. The same applies to spectrophotometric transmission or reflection.

3. Changes of the refractive index under intense laser flux were reported for BaTiO_3 crystals (Reference 5). It might be worthwhile to investigate the method of "writing" and "probe" lasers on BaTiO_3 sputtered films.
4. Large changes of the resistivity were reported in both BaTiO_3 treated in halogens or doped with samarium (Reference 14 and 15). Correlation to optical parameters might be of interest.
5. A major characterization of material suitability for laser hardened applications is the defect areal density; defects arising from the substrate cleaning process, dust, pores due to back sputtering, etc. It was already established and also confirmed in the present work that sputtering synthesis produces pores and probably other defects in the films. It is therefore highly recommended to further examine the BaTiO_3 films by SEM means to establish the relation between the various preparation conditions and the areal density and types of defects.

This would indicate if there are steps that can be taken to improve films quality such as increasing total sputtering pressure, eliminating dust by changing cathode-anode configuration, removing traces of cleaning materials, etc. Or it might be found that sputtering is altogether not a suitable technique for producing films for laser hardened applications.

6. , Though there are several indications for large structural differences between films sputtered below $\sim 700^{\circ}\text{C}$ to films sputtered above $\sim 700^{\circ}\text{C}$, film morphology has not been studied. A cross section SEM examination might reveal the structure, size of grains and orientation (columnar or otherwise) of such things in the sputtered films.

REFERENCES

1. Graham, H. C., Tallan, N. M., and Mazdiyasni, K. S., Microstructure and Electrical Properties of High Purity Barium Titanate, ARL 71-0212, Air Force Systems Command, U.S. Air Force, Wright-Patterson Air Force Base, Ohio, October, 1971.
2. Deshpande, L. V., Joshi, M. B., and Mishra, R. B., "Angle of Polarization and Refractive Indices of BaTiO_3 ," J. Opt. Soc. Am., 70 (9) 1163-1166 (1980).
3. Lawless, W.N., and Devries, R.C., "Accurate Determination of the Ordinary-Ray Refractive Index in BaTiO_3 ," J. Appl. Phys., 35(9) 2638-2639 (1964).
4. Mott, N. F., and Gurney, A. W., Electronic Processes in Ionic Crystals (Oxford University Press, London, 1948).
5. Townsend, R. I., and LaMacchia, J. T., "Optically Induced Refractive Index Changes in BaTiO_3 " J. Appl. Phys., 41 (13) 5188-5192 (1970).
6. McClure, D. J., and Crowe, J. R., "Characterizations of Amorphous Barium Titanate Films Prepared by R. F. Sputtering," J. Vac. Sci. Technology, 16, (2), 311-315 (1979).
7. Pratt, I. H., and Firestone, J., "Fabrication of R. F. Sputtered Barium Titanate Thin Films," J. Vac. Sci. Technology, 8, (1), 256-259 (1970).
8. Panitz, J. K. G., and Hu, C.-C., "Radio-Frequency-Sputtered Tetragonal Barium Titanate Films on Silicon," J. Vac. Sci. Technology, 16, (2), 315-318 (1979).
9. Fan, H. Y., "Infra-Red Absorption in Semiconductors," Rep. on Progress in Phys., 19, 107-111 (1956).
10. Fritzsche, H., "Optical and Electrical Energy Gaps in Amorphous Semiconductors," J. of Noncrystalline Solids, 6, 49-71 (1971).
11. Onton, A., and Mareello, V., "Structure and Excitations of Amorphous Solids," Williamsburg, VA, 1976, AIP Conf. Proceedings, 31, Lucovsky, G., and Galeener, F. L. (Eds.), (American Institute of Physics, New York, 1976), pp. 230-233.
12. Abeles, F., Progress in Optics, Vol. II, Wolf, E. (Ed.), (North-Holland, Amsterdam, 1963).
13. Heavens, O. S., Measurements of Optical Constants on Thin Films, New York, Dover Publications, Inc., 1965.

REFERENCES (Concluded)

14. Janker, G. H., "Halogen Treatment of Barium Titanate Semiconductors," Mat. Res. Bull., 2, 401-407 (1967).
15. Harman, G. G., "Electrical Properties of BaTiO_3 Containing Samarium," Phys. Rev., 106, 1358-1359 (1957).
16. Wohlecke, M., et. al., "Refractive Index of BaTiO_3 and SrTiO_3 Films," J. Appl. Phys. 48 (4) 1748 (1977).
17. Brown, V., "Electrical, Optical and Infrared Properties Vacuum Deposited BaTiO_3 Thin Films," J. Vac. Sci. Tech. 3 (5) (1966).